UNCLASSIFIED

AD NUMBER
AD340140

CLASSIFICATION CHANGES

TO: **unclassified**

FROM: **secret**

LIMITATION CHANGES

TO:

Approved for public release, distribution unlimited

FROM:

Distribution authorized to DoD only; Administrative/Operational Use; 23 OCT 1959. Other requests shall be referred to Defense Atomic Support Agency, Washington, DC.

AUTHORITY

DNA ltr, 24 Jan 1996; DNA ltr, 24 Jan 1996

THIS PAGE IS UNCLASSIFIED

DISCLAIMER NOTICE
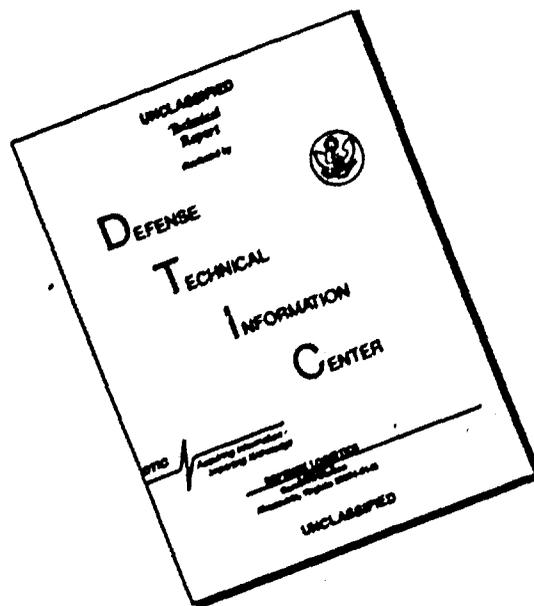
THIS DOCUMENT IS BEST QUALITY AVAILABLE. THE COPY FURNISHED TO DTIC CONTAINED A SIGNIFICANT NUMBER OF PAGES WHICH DO NOT REPRODUCE LEGIBLY.

NOTICE:

Operation REDWING

PACIFIC PROVING GROUNDS

May – July 1956

Project 5.2

IN-FLIGHT PARTICIPATION of a B-52 (U)

Issuance Date: October 23, 1958

HEADQUARTERS FIELD COMMAND, DEFENSE ATOMIC SUPPORT AGENCY
SANDIA BASE, ALBUQUERQUE, NEW MEXIC

Inquiries relative to this report may be made to

Chief, Defense Atomic Support Agency
Washington 25, D. C.

When no longer required, this document may be
destroyed in accordance with applicable security
regulations.

DO NOT RETURN THIS DOCUMENT

(4) NA

SECRET

(5) 127 300

(7) NA

(18) DASA

(20) S-FRD

(9) NA

(19) Rept. No.

(21) Report on

WT-1328

OPERATION REDWING—PROJECT 5.2 [U].

(6)

IN-FLIGHT PARTICIPATION of a B-52 (U)

(8)

(10) by

F. L. Williams, Capt, USAF, Project Officer
and Staff of the Boeing Airplane Company

Wright Air Development Center
Wright-Patterson Air Force Base, Ohio

(11) 23 Oct 59,

(12) 74 p.

(13) — (17) NA

3

SECRET

FORMERLY RESTRICTED DATA

SUMMARY OF SHOT DATA, OPERATION REDWING

Shot Name (Unclassified)	Date EPG	Time (Approximate)	Location	Type	H&N Coordinates (Actual Ground Zero)	Geographic
						° ′ ″
Lacrosse	5 May	0629	Eniwetok Yvonne	Surface Land	124,515 E 106,885 N	11 33 29 162 21 18
Cherokee	21 May	0551	Bikini Off Charlie	Air Drop (4,320 ± 150 ft) Over Water	96,200 ± 100 E 185,100 ± 500 N	11 43 50 165 19 46
Zuni	28 May	0556	Bikini Tare	Surface Land Water	110,309 E 100,154 N	11 29 48 165 22 09
Yuma	28 May	0756	Eniwetok Sally	200-ft Tower	112,155 E 130,604 N	11 37 24 162 19 13
Erie	31 May	0615	Eniwetok Yvonne	300-ft Tower	127,930 E 102,060 N	11 32 41 162 21 52
Seminole	6 June	1255	Eniwetok Irene	Surface Land	75,237 E 149,897 N	11 40 35 162 13 02
Flathead	12 June	0626	Bikini Off Dog	Barge Water	116,768 E 164,094 N	11 40 22 165 23 13
Blackfoot	12 June	0626	Eniwetok Yvonne	200-ft Tower	126,080 E 104,435 N	11 33 04 162 21 33
Kickapoo	14 June	1126	Eniwetok Sally	300-ft Tower	114,018 E 132,295 N	11 37 41 162 19 32
Osage	16 June	1314	Eniwetok Yvonne	Air Drop (680 ± 35 ft) Over Land	126,647 ± 50 E 102,851 ± 50 N	11 32 48 162 21 39
Inca	22 June	0956	Eniwetok Pearl	200-ft Tower	105,300 E 133,540 N	11 37 53 162 18 04
Dakota	26 June	0606	Bikini Off Dog	Barge Water	116,767 E 164,097 N	11 40 22 165 23 13
Mohawk	3 July	0606	Eniwetok Ruby	300-ft Tower	109,737 E 132,165 N	11 37 39 162 18 49
Apache	9 July	0606	Eniwetok Flora	Barge Water	69,227 E 148,063 N	11 40 17 162 12 01
Navajo	11 July	0556	Bikini Off Dog	Barge Water	116,816 E 160,604 N	11 39 48 165 23 14
Tewa	21 July	0546	Bikini Charlie-Dog Reef	Barge Water	99,776 E 164,476 N	11 40 26 165 20 22
Huron	22 July	0616	Eniwetok Flora	Barge Water	70,015 E 148,304 N	11 40 19 162 12 09

4

SECRET

ABSTRACT

The primary objective of Project 5.2 in Operation Redwing was to obtain measured-energy input and aircraft-response data on an instrumented B-52 aircraft when subjected to the thermal, blast, and gust effects of a nuclear explosion.

To accomplish this objective an analysis was performed to determine the effects of nuclear explosions on the B-52 aircraft. This analysis was used in selecting the spatial location for the B-52, relative to a detonation, that would result in the desired aircraft inputs and responses. In addition, the analysis was used in determining the desired locations for the sensing components of the instrumentation system. The B-52 (AF 52-004) was extensively instrumented for participation in Operation Redwing with the major portion of the instrumentation devoted to measuring aircraft responses.

The actual positioning of the B-52 relative to the detonation was accomplished by use of the aircraft Bombing Navigation System (BNS). The B-52 participated in nine shots, including one shot which the aircraft aborted just prior to time zero because of BNS difficulties. The reliability of the instrumentation system was between 95 percent and 100 percent throughout the test program.

The aircraft received up to 110 percent of the allowable limit overpressure, 100 percent of the allowable limit moment on the horizontal stabilizer, and 82 percent of the allowable bending moment of the wing. Except on Shot Huron, aircraft damage was confined to thermal damage on secondary items such as seals, paint on thin skin, and rain-erosion coating on the majority of the exposed plastic surfaces.

During Shots Huron and Tewa the special shoring for both the electronic-countermeasures (ECM) radome and bomb-bay doors was removed to verify that damage to these items would occur in the normal-mission configuration of the aircraft. Prior to Shots Huron and Tewa the ECM radome and bomb-bay doors were shored to achieve a more thorough investigation at near-limit inputs of weapon effects on primary structure. As predicted, during Shot Huron the ECM radome suffered complete failure and the bomb-bay doors received moderate buckling because of overpressure.

The objective established for Project 5.2 was successfully accomplished during Operation Redwing.

It is recommended that the B-52 not participate in future nuclear tests as a weapons-capability aircraft under the delivery conditions stated in the present B-52 Special Weapons Delivery Handbook (Reference 1).

FOREWORD

This report presents the final results of one of the projects participating in the military-effect programs of Operation Redwing. Overall information about this and the other military-effect projects can be obtained from WT-1344, the "Summary Report of the Commander, Task Unit 3." This technical summary includes: (1) tables listing each detonation with its yield, type, environment, meteorological conditions, etc.; (2) maps showing shot locations; (3) discussion of results by programs; (4) summaries of objectives, procedures, results, etc., for all projects; and (5) a listing of project reports for the military-effect programs.

PREFACE

This report constitutes the final reporting of Project 5.2, "In-Flight Participation of a B-52 in Operation Redwing." The B-52 successfully participated in eight shots, collecting approximately three hundred and twenty-five channels of data per shot. Presentation of all collected data would be too voluminous for inclusion in this report and has been presented in its entirety in Wright Air Development Center (WADC) Technical Note 56-446, "B-52B, Operation Redwing Data" (Secret Restricted Data).

Correlation of data collected by the B-52 in Operation Redwing was scheduled for completion in January 1958 and is reported in WADC Technical Report 57-313, "In-Flight Participation of a B-52 in Operation Redwing" (Part I Confidential Restricted Data, Part II Secret Restricted Data).

SECRET

CONTENTS

SECRET

8

SECRET

FIGURES

SECRET

Chapter I
INTRODUCTION

1.1 OBJECTIVE

The primary objective of Project 5.2 in Operation Redwing was to obtain measured-energy input and aircraft-response data on an instrumented B-52 (AF 52-004) aircraft when subjected to the thermal, overpressure, and gust effects of a nuclear detonation. This data will be used to verify or correct the existing "B-52 Special Weapons Delivery Handbook" (Reference 1).

In accomplishing the primary objective, the data collected will be used in satisfying the secondary objectives of determining aircraft modifications pertinent to the improvement of the B-52 nuclear-weapon-delivery capabilities and performing related research for the design of future military aircraft.

1.2 BACKGROUND

The delivery of nuclear weapons presents new problems to the United States Air Force (USAF) with regard to the safety of the delivery aircraft. To insure accurate determination of the maximum safe-delivery capabilities of existing aircraft, as well as future aircraft, the USAF has initiated a research and development program consisting of analytical studies combined with experimental tests.

Initial work of this type consisted of a theoretical study conducted at the direction of the Wright Air Development Center (WADC) to develop methods for the prediction of effects of nuclear explosions on aircraft structures (Reference 2). Thirteen aircraft of various types participated during Operation Greenhouse (1951) to gather data for substantiation of the theoretical study (Reference 3). Subsequent participation during Operations Ivy (1952), Upshot-Knothole (1953), and Castle (1954) provided data for further correlation with the theoretical analysis and for studies which resulted in documents on weapon effects and on the capabilities of several particular USAF aircraft (References 4 through 10, inclusive). Substantial amounts of basic-research data also were obtained for modification and extension of weapon-effect theories. Participation during Operation Redwing was the latest effort to obtain response data on instrumented aircraft.

1.3 INPUT THEORY

A brief review of weapon effects may assist in the understanding of the test procedure and results to follow.

A nuclear explosion is characterized by the rapid release of tremendous energies resulting in high temperature and pressure near the center of the explosion. The escaping radiation and the pressure wave of the initial-nuclear reaction raises the temperature of the surrounding atmosphere to incandescence, forming a fireball which in turn releases the thermal radiation which is of interest in determining aircraft capabilities. The high pressures result in the formation of a blast wave preceded by a high-velocity shock front. The energy release from the explosion also includes the emission of nuclear radiation and radioactive particles.

1.3.1 <u>Thermal.</u> The thermal radiation from the fireball is neither constant in intensity nor uniform in color temperature with time. The length of the heat pulse produced varies with the size of the explosion, although it has a characteristic time-intensity variation, rising steeply to a maximum, then decaying more slowly over the major portion of the pulse duration. The thermal radiation incident on a receiver surface is a function of the size of the explosion, irradiance history, spectral distribution of the radiation, atmospheric attenuation and scatter, albedo, and position and orientation of the receiver as a function of time.

Thermal radiation was computed by the methods outlined in Reference 11, which takes into consideration fireball shape, atmospheric attenuation and scatter, and earth-surface albedo. In accordance with Reference 11, the emission of the radiant-thermal energy is divided into an upper and lower phase of fireball growth and is briefly summarized in the following equation:

$$Q_h = Q_l \cos \theta_l + Q_u \cos \theta_u + Q'_l + Q'_u$$

Where: Q_h = total thermal energy perpendicular to a horizontal receiver, cal/cm^2

   Q_l = direct thermal energy to a receiver normal to a ray through ground zero, lower phase, cal/cm^2

   Q_u = direct thermal energy to a receiver normal to a ray through the center of the fireball, upper phase, cal/cm^2

   Q' = reflected energy perpendicular to a horizontal receiver, cal/cm^2

   Subscript l and u are lower and upper phase, respectively.

θ_l, θ_u = the angle between the vertical through the fireball center and the radial line from the fireball center to the receiver, lower and upper phase, respectively.

The procedures for computing the respective components of the above equation are quite extensive. See Reference 11 for these details.

The effect of aircraft movement was considered by computing the portion of radiation available to the aircraft (at successive locations along the flight path) which resulted in an effective thermal pulse received by the aircraft. The method is described in detail in Reference 12. An average source color temperature of 3,000 K was assumed for surface bursts and 6,000 K for air bursts as recommended in Reference 11.

1.3.2 <u>Overpressures and Material Velocity.</u> The blast wave emanating at high velocity from a nuclear detonation produces a material velocity preceded by a shock front and increases the pressure, density, and temperature of the atmosphere through which it passes. The material velocity is assumed to be in a direction normal to the shock front, the shape of which is influenced by atmospheric refraction.

At a fixed point in space, the atmospheric quantities remain undisturbed until shock-front arrival. At shock arrival, the overpressure and material velocity increases practically instantaneously to their maximum-positive-phase values. After passage of the shock front, the overpressure and material velocity decrease to zero, enter a negative phase of lesser peak magnitude, and finally decay to steady-state values.

The quantities associated with the shock wave have been determined from predictions

12

SECRET

of peak overpressures at points in space. The overpressure predictions have been derived from the normalized composite free-air overpressure data presented in Reference 13, modified for altitude by the approximate method set forth in Reference 14. The time of arrival of the shock front at a point in space was found by integration of the reciprocal of the shock-wave velocity with respect to time along a straight line path from the burst center. The direction of the material velocity was determined by measurement from the isotime curves.

With the overpressure at a point in space known, the material-gust velocity was determined by means of Rankine-Hugoniot relationships.

1.3.3 Nuclear Radiation. It was recognized that nuclear radiation emitted from nuclear detonations might be significant as a physiological danger to aircraft crews and could be an aircraft-positioning problem. In the fall of 1955, a meeting was held between WADC and Armed Forces Special Weapons Project (AFSWP) personnel at Kirtland Air Force Base, New Mexico, to determine the criticality of nuclear radiation for effects aircraft in Operation Redwing. It was determined that nuclear radiations were insignificant for the planned positions of the B-52 effects aircraft in this operation and for any delivery condition.

1.4 RESPONSE THEORY

Aircraft responses to the weapon effects mentioned in the previous section are described below.

1.4.1 Thermal. The primary response of the aircraft to incident-thermal radiation is a temperature rise in the exposed elements. The magnitude of the temperature rise is dependent upon the amount of the incident energy absorbed; the time during which the energy is absorbed; the mass, thermal capacity and physical arrangement of the material exposed; and the heat lost through conduction, convection, and radiation.

Two types of thermal responses on the structure were considered. One response was the temperature rise on outside thin-skin elements sufficiently free of heat sinks that they could be treated as being free of conduction-heat losses. Reradiation losses were considered insignificant. The second response was the temperature rise and the resultant induced strain where the skin backup structure caused a significant temperature gradient.

By assuming that conduction and reradiation losses have a negligible effect on the temperature rise in an exposed thin-skin panel, the heat balance equation may be reduced to the following simplified form:

$$dT_S \text{ (cwb)} = \left[\alpha q - h_c (T_S - T_{aw})\right] dt$$

The time-temperature history of a thin-skin panel was determined by converting the above heat balance equation to a finite-difference form and performing successive solutions. The equation may then be written as:

$$T_{s_{i+1}} = T_{s_i} + \frac{\Delta t}{cwb} \left[\alpha q_{i+1} - h_c (T_{s_i} - T_{aw})\right]$$

Where: c = specific heat of the skin material, Btu/lb-°R

w = specific weight of the skin material, lb/ft^3

13

SECRET

b = element thickness, ft

T_s = element temperature, °R

α = surface absorptivity coefficient, dimensionless

q = rate of heat intensity normal to skin surface as a function of time. Assumed constant over the time interval i, Btu/ft^2-sec

t = time, sec

h_c = forced convective-heat-transfer coefficient, Btu/ft^2-sec-°R

T_{aw} = adiabatic wall temperature = $T_\infty(1+0.18M^2)$, °R

T_∞ = absolute ambient temperature, °R

M = mach number, dimensionless

i = iteration number, dimensionless

The forced convective-heat-transfer coefficient for a turbulent-boundary layer was calculated by the equation,

$$h_c = \frac{5.889 \times 10^{-6} (VP)^{0.8}}{(X_l)^{0.2} (T_f)^{0.5}}$$

Where: V = aircraft velocity, ft/sec

P = ambient atmospheric pressure, lb/ft^2

X_l = distance from leading edge of surface, ft

T_f = film temperature = $(T_{aw} + T_s)/2$, °R

The thermal radiation falling on the external surface of a skin-stiffener segment results in a temperature gradient through the skin and stiffener with an initial heat flow as shown in Figure 1.1.

Points of maximum temperature occur in the skin between stiffeners, and no appreciable heat flows across this boundary. If the stiffeners are of equal mass, as is the usual case on the aircraft structure, the heat boundaries will occur at the midpoint of the free skin between stiffener flanges and will remain stationary with time during a transient-heat input. Under these conditions the skin-stiffener segment between these boundaries may be treated as a unit without regard to the adjacent structure. Furthermore, since the change in mass of the segment with respect to length along the stiffener axis is small, it may be assumed that the heat flow in this direction is negligible and the temperature solution may be made for a segment of unit length.

In the temperature solution, the skin-stiffener segment is divided into elements as shown in Figure 1.1 and a heat balance equation is written for each element. The equations are similar to those used for the isolated thin-skin element except for the addition of conduction terms. The same assumption regarding reradiation losses apply. The general heat-balance equation for each element is given in finite-difference form as:

14

SECRET

$$cwbA\left(T_{N_{i+1}} - T_{N_i}\right) = \alpha\,q_{i+1} \times A \times \Delta t + \frac{KA'\,\Delta t\,(T_{N-1} + T_N)_i}{(l_{N-1} + l_N)/2}$$

$$-\frac{KA'\,\Delta t\,(T_N - T_{N+1})_i}{(l_N + l_{N+1})/2} + K'A\,\Delta t\,(T_{N-1} - T_N)_i$$

$$- K'A\,\Delta t\,(T_N - T_{N+1})_i - h_c A\,\Delta t\,(T - T_{aw})_i$$

Where: A = surface area of the element = ld, ft^2

A' = cross-sectional area of element normal to direction of heat flow = bd, ft^2

K = thermal conductivity of material, Btu/ft-sec-°F

K' = thermal conductance across a joint, Btu/ft^2-sec-°F

l = length of element, ft

d = width of element, ft

b = thickness of element, ft

N = sequence number of element increasing in direction of heat flow

Other terms are the same as defined in the preceding thin-skin equation.

The stresses induced in the skin stiffeners by the thermal gradient may be computed from the following equation as derived from the analysis reported in Reference 26.

$$f_{th_N} = \theta E \left[\frac{\Sigma A''\,\Delta T}{\Sigma A''} + \frac{\Sigma A''y\,\Delta t}{\Sigma A''y^2} \times y_N - \Delta T_N \right]$$

Where: f_{th_N} = thermal stress at element N, psi

θ = coefficient of thermal expansion, in/in-°F

E = modulus of elasticity, psi

A'' = cross-sectional area of elements in a plane normal to the stiffener axis, in^2

T_N = temperature rise of element N

y = distance from neutral axis of the skin-stiffener segment to any element, in

1.4.2 Overpressure and Material Velocity. An aircraft encountering the blast wave from a nuclear detonation is immediately enveloped by an overpressure and is subjected to time-dependent aerodynamic forces and an ensuing motion which may critically affect its structural integrity, stability, or control. Although the overpressure and material

15

SECRET

velocity affect the aircraft simultaneously, they are usually considered separately since their structural responses are different.

The major effect of overpressure is to cause local damage to such items as bomb-bay doors, wing flaps, radomes, access doors, and thin skin.

The aircraft response to the material velocity, or gust, following the blast wave of a nuclear explosion is primarily one of aeroelastic response to the incremental airloads induced by the gust. The material velocity induces a load increment because of a nearly instantaneous angle of attack change. If the gust is from behind and below, the aircraft is caused to accelerate upward and to pitch nose downward. The resulting aircraft upward-velocity component serves to reduce the effective-vertical component of the gust and, hence, the incremental angle of attack. The pitching also decreases the angle of attack. Therefore, the ensuing motion tends to alleviate the net-aerodynamic forces which caused it. Eventually, an equilibrium condition is attained as the material veloc-
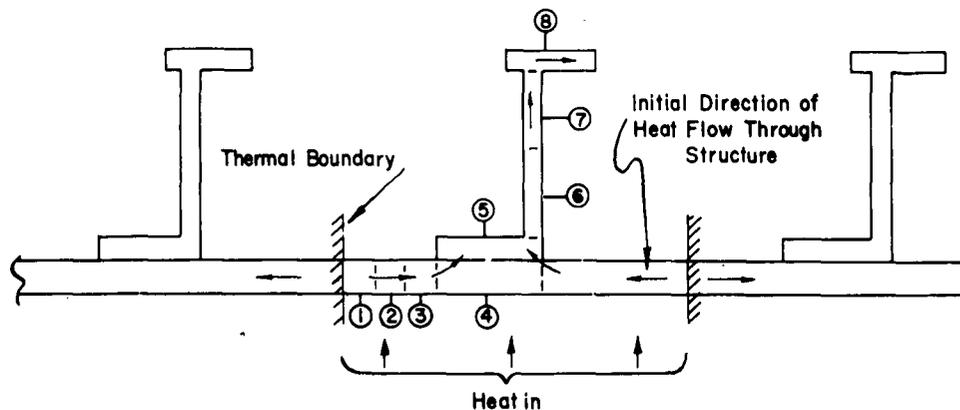
Figure 1.1 Typical skin-stiffener segment for thermal analysis.

ity decays from its initial-peak value. For the methods employed in Reference 1 and Operation Redwing positioning calculations, the aircraft was assumed to be flying straight and level tail-on to the burst at the time it was overtaken by the nuclear-blast wave. The shock front, considered to be a plane surface, passes over the wing from behind and below and moves at a high velocity relative to still air. The material velocity behind the shock front and moving in the same direction as the shock front combines with the air-craft velocity to result in a decreased aircraft-relative velocity at an increase in angle of attack. This shift in relative velocity and angle of attack is practically instantaneous upon shock arrival and results in a sharp increase in airload and load factor. The same concept will generally apply to the tail, with minor differences to account for downwash and tail angle. The analysis is complicated, however, by the changes in pressure, den-sity, and temperature which accompany the blast wave. These changes affect the equiv-alent velocities upon which aerodynamic lift depends.

For the investigation of aircraft response to blast effects, an adaptation of a quasi-static condition with the use of dynamic magnification and gust-alleviation factors was used which gave realistic results without recourse to the prohibitively long-calculation procedures of a more exact solution. This approach utilized, as a starting point, the quasi-steady aerodynamic assumption of instantaneous attainment of peak lift to com-pute a maximum quasi-steady vertical load factor increment. The effects of lift growth, rigid-body motion, and dynamic-elastic motions were then brought into consideration by

16

SECRET

applying to the maximum quasi-steady vertical load factor increment a gust alleviation factor, K_g, and a dynamic magnification factor, D.

This approach may be illustrated in equation form as,

$$M_G = M_1 + K_g D(\Delta M)$$

Where: M_G = final bending moment

M_1 = preshock, level-flight bending moment

ΔM = change in bending moment from preshock values as determined from a quasi-static load concept

The product of dynamic magnification and gust-alleviation factors, $K_g D$, used for the wing and horizontal stabilizer of the B-52 in this operation represents conservatively-selected envelopes based upon theoretical values calculated in detail. Calculations were made using analog equipment for a number of different cases involving weapon and aircraft parameters. For the critical portion of the wing, the inboard section, a $K_g D$ value of 1.4 was used. A $K_g D$ value of 2.0 was used for the horizontal stabilizer. As noted in Section 4.7, it was necessary to adjust these values, generally downward, as a result of measured data as the program progressed.

The quasi-static incremental moment, ΔM, may be determined from known-load parameters and calculated incremental-load factors. This is defined in equation form as,

$$\Delta M = (M_2 - M_1)_{n=1} + \frac{\partial M}{\partial n} \Delta n_w + \frac{\partial M_d}{\partial n} \Delta n_t$$

Where: M_1 = preshock, level-flight bending moment

M_2 = level-flight bending moment in postshock aerodynamic regime

$\frac{\partial M}{\partial n}$ = partial derivative of net beam bending moment with respect to load factor (Mach No. and 2 held constant)

$\frac{\partial M_d}{\partial n}$ = partial derivative of dead weight beam bending moment with respect to load factor (Mach No. and q held constant)

Δn_w = incremental aircraft vertical load factor due to gust load on the wing

Δn_t = incremental aircraft vertical load factor due to gust load on the tail

It will be noted that the tail incremental-load factor affects only the bending moment due to the dead weight of the wing and not the aerodynamic quantities. The final expression for the postshock bending moment becomes

$$M_G = M_1 + K_g D \left[(M_2 - M_1)_{n=1} + \frac{\partial M}{\partial n} \Delta n_w + \frac{\partial M_d}{\partial n} \Delta n_t \right]$$

1.5 AIRCRAFT LIMITS

The critical limits on various components of the B-52 used for positioning the air-

17

SECRET

craft in Operation Redwing were determined by analyses, specimen laboratory tests, and aircraft-static tests.

1.5.1 Thermal. To determine limiting-thermal capabilities for structural alloys and plastics with and without various types of paint and primers, tests were performed at Boeing Airplane Company (BAC) and Naval Radiological Defense Laboratory (NRDL) (Reference 15). In addition, miscellaneous items of aircraft equipment such as seals, vents, etc., were also tested at BAC (Reference 16). As a result of these tests and studies on the effects of repeated thermal inputs on the aircraft-material properties, an allowable temperature of 600 degrees Fahrenheit was established on magnesium and aluminum thin-skin structures. Lower thermal capabilities of non-critical re-placeable items, as far as aircraft safety was concerned, were not used as limiting considerations for positioning the aircraft.

1.5.2 Overpressure. Critical static overpressures were obtained by subjecting the static-test aircraft to internal negative-air pressures (Reference 17). Since the dynamic effects of an instantaneous overpressure buildup caused by a nuclear detonation could not be duplicated in the static test, a dynamic magnification factor was used with the static test results to determine the allowable free-air overpressure. With a mag-nification factor of 1.25, the basic-aircraft-allowable-free-air overpressure was determined to be 0.8 psi. In the static test, two exceptions to this allowable limit were found. A magnification factor of 1.67 was believed to be realistic for the ECM radome because of size and for the bomb-bay doors because of their size and edge support. On this basis, the allowable-free-air overpressure for the ECM radome was determined to be 0.24 psi and for the bomb-bay doors, 0.34 psi. In order to evaluate the aircraft-overpressure capabilities at the test site, the ECM radome and bomb-bay doors were shored to raise their capabilities to at least 0.8 psi. The shoring was used in all but the last two B-52 test-shot participations.

Analytical studies indicated the possibility of the inboard-wing flaps being critical for overpressure loads. The most critical item was crushing in the flap-track-rib chords, caused by the high-reaction load of the aft-flap bumpers. The aft-bumper load was alleviated by the installation of an additional set of bumpers on the flap spar at each flap track. Using the flap rib and spar strengths as noted in the stress analysis of this component (Reference 18), the allowable-free-air overpressure of approximately 0.5 psi was then computed.

1.5.3 Material Velocity. Aircraft limits cannot be stated in terms of material velocity alone because of the influence of other factors, such as aircraft orientation, altitude, and velocity. The incremental airloads resulting from the material velocity, described in Section 1.4.2, combine with steady-state-flight loads to produce struc-tural loads which can be compared with limits stated in terms of allowable loads on the various structural components. The wing, stabilizer, and fuselage-allowable loads were determined during the B-52 static-test program. At the critical locations, allow-able loads were as follows: Wing Station 444 bending moment, 56.9×10^6 in-lb; Sta-bilizer Station 300 bending moment, 0.78×10^6 in-lb; total tail load, 126,000 lb; and Body Station 1332 vertical shear, $\pm 120,000$ lb. The load ratios shown in Chapter 3 are based on these allowable shears and moments.

18

SECRET

Chapter 2
PROCEDURE

2.1 OPERATIONS

2.1.1 Aircraft Preparation. Concurrent with the decision in 1954 for participation of a B-52 in Operation Redwing, a B-52 was in the process of being instrumented for a flight-load-survey program. The flight-load instrumentation partially fulfilled the Operation Redwing requirements, so the same aircraft was used in both programs. Installation of additional transducers and the majority of the wiring for transducers to be later installed was accomplished during the instrumentation phase of the flight-load survey.

The initial instrumentation was accomplished during 1954. Calibration of all flight-load-survey transducers and those installed for Operation Redwing was accomplished during February and March of 1955. A description of the calibration is contained in Reference 19.

During the summer of 1955, familiarization flights were conducted by the USAF crew for Operation Redwing. In September 1955, the majority of the remaining instrumentation was installed and calibrated. In November and December, 1955, simulated Operation Redwing missions were flown with the complete flight crew. The B-52 then entered a final lay up for maintenance, modification, painting, final instrumentation installation and repair, and preparation for overseas movement. The aircraft was accepted by the USAF in February 1956.

All aircraft instrumentation was installed, calibrated, and maintained by the Boeing Airplane Company under contract with Wright Air Development Center (WADC) in the United States and at the test site. Aircraft maintenance was performed by Boeing personnel until departure for the test site, after which WADC personnel assumed maintenance responsibility. Project 5.2 organization and its relationship to Program 5 is shown in Appendix A.

2.1.2 Shot Participation. The names and yields of shots on which the B-52 participated are noted in Table 3.1. The maps of the Bikini and Eniwetok atolls and the Summary of Shot Data Table, which comprise the frontispiece, show all shots detonated during Operation Redwing as well as their location, time, and type of detonation.

2.1.3 Operational Procedures. The operational procedures used during Operation Redwing were, for the most part, adapted from experience gained in Operations Ivy, Upshot-Knothole and Castle. For each shot, the aircraft was positioned on the basis of the positioning yield. Because of the state of the art in prediction of nuclear-weapon effects on aircraft, it was necessary to position the aircraft for approximately 80 percent of limiting criteria until the validity of the prediction methods could be established. Upon satisfactory correlation between the prediction methods and test results, the aircraft was positioned to receive higher percentages of allowable-limit wing load, stabilizer load, overpressure, or temperature. The actual prediction methods were refined from shot to shot, as measured data was analyzed.

The procedure is illustrated in Figures 2.1 and 2.2 which show superimposed response curves for the various weapon effects. Two figures have been used for clarity. It should
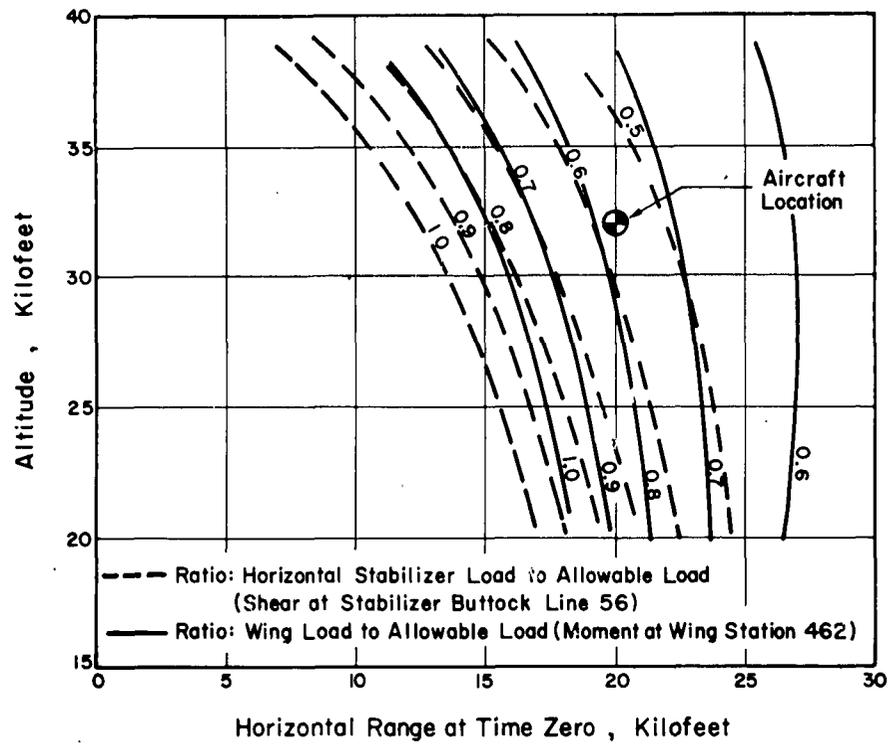
Figure 2.1 Wing and tail load positioning chart.
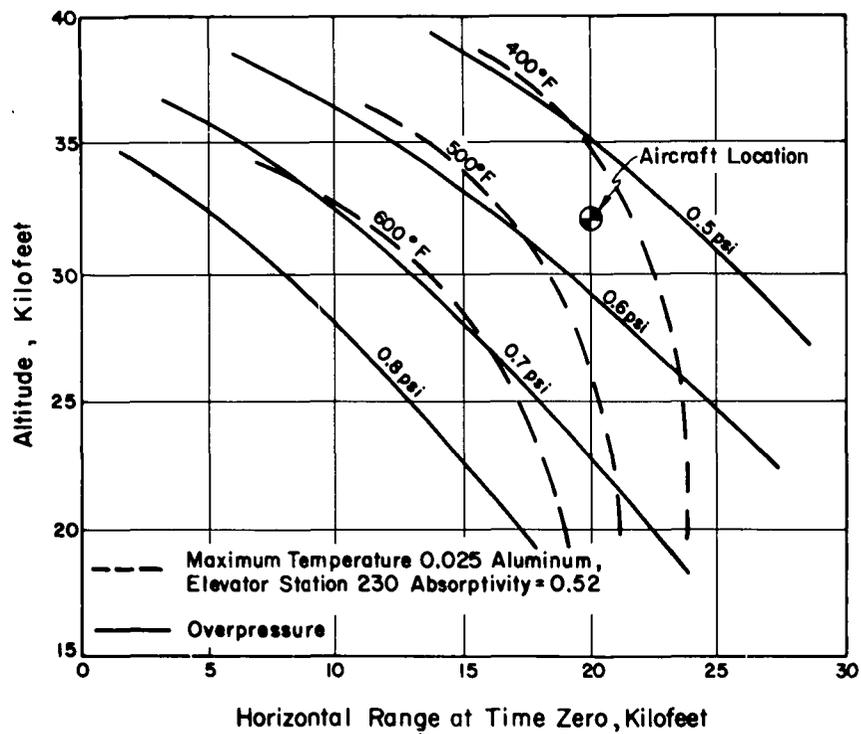
Figure 2.2 Maximum temperature and overpressure positioning chart.

20

SECRET

be noted that while both figures have an abscissa of Horizontal Range at Time Zero for comparative purposes, the effects shown in Figure 2.1 and the overpressure shown in Figure 2.2 will occur at the time of shock arrival, some time after time zero. The aircraft velocity must be assumed constant to construct such charts, since the time of shock arrival at any point in space is a function of overpressure for a given weapon yield. In Figure 2.1 it can be seen that the proposed-aircraft location would have resulted in the development of 57 percent of the allowable-stabilizer shear at Buttock Line 56, and about 77 percent of the allowable--bending moment at Wing Station 462. From Figure 2.2 it can be noted that the position indicated would have produced a temperature of approximately 430 degrees Fahrenheit in the thin-aluminum skin of the elevator and that the aircraft would have to withstand an overpressure of 0.55 psi. It is also apparent from the figures that the aircraft location could be adjusted to keep one effect constant while varying others.

Figures 2.1 and 2.2 are presented as an example and the curves shown are not necessarily those for the most critical effects. As testing progressed, it became evident that the bending moment at Stabilizer Station 300 was one of the more critical items. In subsequent charts similar to those of Figures 2.1 and 2.2, therefore, curves showing the criticality of Stabilizer Station 300 were included.

Aircraft location was also influenced by operational factors. It was desired that the aircraft be within 5,000 pounds of a gross weight of 270,000 pounds and that the center of gravity be close to 26 percent of the mean-aerodynamic chord at the time the aircraft was subjected to weapons effects. This requirement was dictated by the fact that 270,000 pounds represented a reasonable over-target weight for a bombing mission, and because base-stress-level-load data had been taken at this weight.

A minimum test altitude of 20,000 feet was established because of high fuel consumption at lower altitudes and limited take-off gross weight determined by runway length. A maximum altitude of 41,000 feet was established because of limits to aircraft-acceleration capabilities at higher altitudes that would increase the possibility of an aborted run-in if the airplane were behind schedule.

After arriving at a decision as to the desired aircraft responses for a particular shot, a position in space at time zero was calculated as outlined above, which would subsequently result in those responses. The altitude was coordinated with all other participating aircraft and the flight path arranged to avoid restricted areas. The positioning data were then presented to Task Groups 7.1 and 7.4 for approval.

A detailed flight plan was prepared for each shot to assist the flight crew in positioning the aircraft at the desired altitude, horizontal range, orientation, and airspeed with the desired gross weight and center-of-gravity location at shot time.

The desired aircraft locations in space were attained by the use of a modified radar bombing-navigation system (BNS). This modification added an auxiliary positioning computer (APC) to the radar ME-5 computer. A brief description of the use and operation of this system in positioning the aircraft is given below.

The desired location in space at time zero was set into the BNS in terms of north and east offsets relative to ground zero. This allowed the navigator to position the aircraft at the desired location by actually sighting on the ground-zero target. While the bomb-sight cross hairs were held on the target during the run-in, the ME-5 computer calculated the time-to-go (that is, the remaining time before the aircraft would reach the desired location). A ground transmitter broadcast a radio tone from the weapon-timing sequences to the aircraft at exactly time zero minus 6 minutes. The radio tone triggered a time-standard oscillator in the APC system. The APC then compared time-to-go with time-to-detonation and presented this comparison (on dials) to the pilot and to the navigator. If these two times were equal, the dials read zero

and the aircraft would reach the desired location at time zero if its speed were maintained. If a difference existed between the two times, the dials indicated the aircraft was early or late in terms of seconds. This indication allowed the pilot to adjust the aircraft speed to compensate for the difference between the two times so as to arrive at the desired position at time zero.

The aircraft was flown to the test area and four to six positioning timing runs were made (Figure 2.3). Upon completion of the timing runs, a wind box was flown to allow the navigator to arrive at the initial point at approximately 6 minutes prior to time zero on the final run.

Prior to each flight, a complete preflight inspection and checkout of all instrumentation was accomplished. This preflight check consisted of balancing, aligning, and standardizing of each channel of information, and titling the film of each camera. During this check, malfunctioning gages were replaced with stand-by gages or were repaired. On each flight, an in-flight calibration check and zero references were ob-
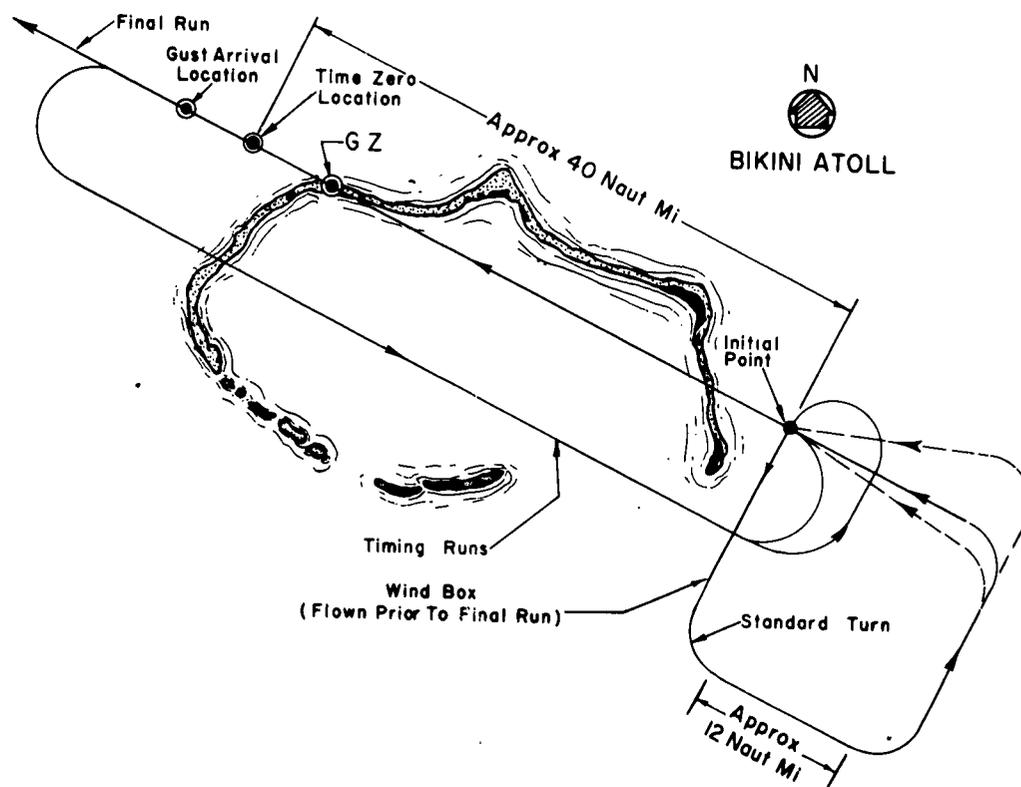
Figure 2.3 Typical flight pattern.

tained through the use of an sinusoidal roller-coaster maneuver prior to time zero and shortly after shock arrival. Also, an instrumentation standardization was performed prior to time zero and shortly after shock arrival. All instrumentation was operated by the flight test engineer at the electronic-countermeasures (ECM) operator's station. After landing, a complete postflight check of all instrumentation, similar to the preflight, was accomplished. Any gages that malfunctioned during the postflight inspection

22

SECRET

were carefully examined during the test portion of the data record in order to eliminate incorrect data.

In addition to the standard aircraft equipment, a spare ultra-high frequency (UHF) radio (with transfer switch at the pilot's station) was provided and two very-high frequency (VHF) radios were used for ground communications and APC signals.

Curtains for the protection of crew members were installed on all crew compartment windows. These areas were not exposed directly to the bursts, but it was anticipated that a sufficient amount of radiation might be received from cloud reflection and atmospheric back-scatter to cause injury to crew members or equipment. The curtains were constructed of one layer of white cotton duck (MIL-D-10861), facing the radiation, sewn together with one layer of aluminized-vinyl-coated cotton twill (MIL-C-7642 Type I), with the vinyl facing away from the crew. The curtains were mounted so they could be drawn over the windows when in the effects area and retracted to the window edge when not in use. Electrical wiring in the window-frame area, which was not shielded by the curtains, was protected by a wrapping of aluminum foil.

2.2 INSTRUMENTATION

Skin temperatures were measured by means of 85 thermocouples located in the surfaces of the left wing, left horizontal stabilizer, and lower surface of the fuselage. Ten of the thermocouples were unique in that they were used to determine convective cooling effects. In addition, a total of twenty-five calorimeters and two radiometers were used to measure radiant exposure and irradiance.

Complete flight-load data for moments, shears, and torsions were obtained by instrumenting the wing, body and tail structure with strain gages in uncombined-single and combined-multiple bridges. In addition, single and multiple uncombined strain gages were used to measure stresses.

Additional aircraft instrumentation included gyros to measure the angles of roll and pitch, pressure transducers to measure overpressures, accelerometers for measurement of angular and translatory-structural component accelerations, and control-surface-position transducers.

Recording oscillographs and cameras supplied time-histories of all sensing transducers, aircraft position, and other pertinent data. Instrumentation locations are diagrammed in Appendix B.

2.2.1 Thermal Transducers. The calorimeters and radiometers used on the B-52 in Operation Redwing were made by Naval Radiological Defense Laboratory (NRDL), except for two calorimeters at Body Station 1500 which were made by Boeing. Twenty-five calorimeters and two radiometers were available throughout the aircraft to measure the thermal-spectral distribution and radiant exposure at the aircraft (Figure B.6 in Appendix B).

Sixteen of the calorimeters were mounted in a box on the tail turret for measurement of the thermal radiation through filters in seven wave-band regions. These instruments were supplied at the request of, and to obtain data for, the Air Force Cambridge Research Center (AFCRC), Project 5.7. One was referenced to an ice bath for heat-capacity corrections. Two radiometers in the same box measured the irradiance. Two calorimeters were located inside the ECM radome forward of the forward wheel-well to investigate thermal-radiation transmission through the radome. One was mounted above a painted area and the other above an unpainted area. To record the radiant exposure normal to the lower side of the fuselage, three 160-degree-view calorimeters were placed at Body Station 650. Two units at Body Station 1500 were

23

used to determine the convective-cooling effect. Two additional calorimeters recorded the thermal radiation reaching the crew compartment. One was placed inside the cockpit behind the white-thermal curtain and was referenced to an ice bath. The other was placed outside the windshield on top of the nose and was referenced to outside-air temperature.

Eighty-five butt-welded copper-constantan thermocouples were installed in the B-52 to measure thermal responses (Figures B.2, B.3, B.4, B.6, and B.8). The thermocouples, with the exception of those in laminated glass, were held in place by means of small dural screws and nuts. Thermocouples were arranged on stiffeners in several areas to measure heat gradients through the structure. Duplicate thermocouples were installed at each location as a stand-by, and all thermocouples were referenced to the ice bath.

To investigate the effects of cooling by the airstream, ten thermocouples were mounted on the under side of the outboard portion of the left wing in two chordwise rows of five thermocouples each. The thermocouples in one row were isolated from the airstream by transparent-fuse-quartz covers, and the thermocouples in the other row were uncovered. Six copper-constantan thermocouples were installed in the sandwich-constructed ECM radome, located forward of the forward wheel-well, to determine radome-temperature gradient. They were installed in two sets of three, one set on an unpainted portion of the radome and the other set on a painted portion. Each set consisted of a thermocouple on the outer surface of the outer lamina, one on the inner surface of the outer lamina, and one on the inner surface of the inner lamina. Six additional thermocouples were similarly installed as stand-bys.

Standard iron-constantan and chromel-alumel temperature probes recorded inlet, low compressor, high compressor, burner, and tailpipe temperatures of the No. 6 engine.

Thirty strain gages were installed on the lower surface of the wing to measure spanwise-thermal strain. Ten strain gages were installed on the lower surface of the horizontal stabilizer, five to measure spanwise-thermal strain and five to measure chordwise-thermal strain. In addition, duplicate strain gages were installed as standbys (Figures B.2 and B.7).

2.2.2 Load Transducers. Fifty-eight load bridges (plus a complete set of stand-by bridges) were installed to measure shears, moments, and torsions on the wing, fuselage, and tail surfaces (Figures B.1, B.3, B.5, and B.7). Each load bridge consisted of one prime-strain-gage bridge attenuated electrically with two or more other bridges in such a manner that the combined bridge was sensitive only to one type of load. The selection of attenuating resistors resulted from a ground calibration of the instrumentation installed in the aircraft. All load bridges were temperature compensated. Prior to Operation Redwing, an extensive flight-load-survey program, utilizing this instrumentation, was conducted on the aircraft (Reference 20).

The strain gages used in the combined circuits were Baldwin SR-4, paper dual-lead type AD-6, paper wrap-around type A-13-1, or bakelite temperature-compensated type EBDF-13D. They were installed using Baldwin SR-4 cement on the paper gages and Shell Oil Company Epon VI on the bakelite gages. Sealing against high humidity was accomplished by applying coatings of neoprene, Minnesota Mining compound EC776, and Products Research Company PR 1201 in fuel areas. In other areas protection was provided with neoprene and PR 1201 or PR 1201 alone.

In addition to the combined load bridges noted above, sixteen stress bridges (ten on the upper surface of the wing, one each on the fin and left stabilizer, and one on each of

the four fuselage longerons at Body Station 710) were installed at intermediate points relative to the load-bridge stations. A complete set of stand-by gages was also installed for each stress bridge (Figures B.1, B.3, B.5, and B.6). These gages were installed so that they were relatively insensitive to local bending or to loads other than primary-beam bending. They were used as a check on spanwise-moment variation as obtained by the load bridges. Their responses to load were checked during the ground calibration.

The strain gages used in the uncombined bridges were Baldwin SR-4 felt-backed-paper types A-3 and A-5-1 or bakelite temperature-compensated type EBDF-7D or EBDF-3D. All gages were attached and sealed as noted above.

Analytical studies indicated the possibility of the inboard-wing flaps being critical for overpressure loads. As a result of this study, the B-52 effects aircraft was equipped with a set of support bumpers on the upper surface of the inboard flaps at the intersections of the flap-track centerlines and the flap spar. Prior to Shot Flathead, the bumper at Wing Station 398 was replaced with a strain-gage-instrumented bumper calibrated to measure the flap-track reaction to the overpressure load on the flap.

Structural deflections (bending and torsional) were photographed by two cameras located above the upper-wing surface on the centerline of the fuselage (Figure B.6). Targets were mounted on the upper surface of the wings, forward edge of the fin, and on the horizontal-tail surfaces for photographic reference. The targets were illuminated for positive identification and night operations.

2.2.3 Overpressure and Acceleration Transducers. Fifteen Statham-type-pressure transducers were located throughout the aircraft for the primary purpose of measuring time-intensity histories (Figures B.6, B.8, and B.9).

Four of these transducers were in the left stabilizer, one was in the left side of the fin, and ten were in the fuselage. Pressure transducers in the vertical tail, lower-aft portion of the body, and lower-forward portion of the body were used to evaluate the rate and direction of shock propagation over the length of the body and tail. Sideslip angle was measured by the differential pressure between static ports on each side of the aircraft fuselage.

Body and fin overpressure transducers were of the unbonded strain-gage, temperature-compensated type. The dynamically balanced Statham P-96 and the flush-diaphragm Statham P-81 differential-pressure transducers were used for body and tail-skin installations. Both these units had low sensitivity to linear accelerations. However, the P-96, which had a double bellows, was somewhat sensitive to angular vibration. The range of the P-96 was ± 3 psi and its natural frequency was 600 cps. The P-81 had a ± 5 psi range and a natural frequency of 5,500 cps. Tubing connections were made so that only the gust overpressure was recorded. This was accomplished by venting the pressure-input side to the pressure-pickup point and the reference side to the same point through a normally-open solenoid valve. The valve was closed just prior to the test, thus giving as a reference the ambient pressure prior to shock arrival.

Engine response to the shock wave and gust was recorded by pressure transducers at various locations throughout the No. 6 engine (Figures B.3 and B.4). Twelve transducers were located at the engine intake to obtain a history of the intake-pressure distribution. Internal-engine pressures were also measured at the low-pressure-compressor outlet, the high-pressure-compressor outlet, burner section, and turbine exhaust.

The inlet pressures were measured with Statham P6TC temperature-compensated ± 2 psi differential-pressure transducers, referenced to the shielded pitot prior to gust. Engine-internal pressures were measured with Statham type P-24 temperature-

compensated absolute-pressure transducers. Pressure ranges were 50, 100, and 200 psi. The transducers were all installed forward of the transverse firewall, with tubing to pick up the burner and tailpipe pressures.

Fourteen angular and twenty-two linear accelerometers were located in the tail, fuselage, wings, and engine nacelles to obtain data on aircraft response to the shock wave and material velocity (Figures B.1, B.3, B.5, and B.7). Angular accelerations about the pitch axis were measured. Two vertical accelerometers mounted near the aircraft center of gravity were used to record normal acceleration on separate oscillographs. A third accelerometer, similarly mounted, was connected through a servo amplifier to a sensitive indicator at the pilot's panel. This latter instrument was used by the pilot in accomplishing in-flight calibration-check maneuvers.

Linear accelerations were measured with Statham unbonded-strain-gage, controlled-temperature, temperature-compensated,type A-30 and A-33 accelerometers mounted on a rotatable base which was used for functional and preflight checks. One channel used a Genisco controlled-temperature, potentiometer-type accelerometer. This instrument was installed at the aircraft center of gravity and was chosen for its low-frequency response. The angular accelerometers were Statham temperature-compensated, unbonded-strain-gage type AA-14 transducers.

2.2.4 Control Surface Position Transducers. Left aileron, left and right inboard spoiler, left and right elevator, stabilizer, and rudder positions were measured by seven angular-position transducers. An angular-position transducer consists of a cylindrical housing which contains a thin steel blade rigidly connected to one end of the case and to a protruding shaft at the other end. Baldwin SR-4 bonded-paper strain gages are installed on opposite sides of the blade at 45 degrees with its axis and connected to have an output only for torsional deflections of the blade. The housing is attached to the aircraft on the hinge line of the control surface. The shaft is connected to a forked arm which fits around a pin on the control surface so that there are no thrust or side loads on the transducer. The transducer is inherently linear, temperature-compensated, and treated in the circuit as a simple-strain-gage bridge. This instrument was developed and fabricated by the Boeing Airplane Company.

2.2.5 Cameras. Ten type N-9 Gun-Sight-Aiming-Point (GSAP) cameras were used in the airplane (Figure B.6). Six were mounted in the tail turret adjacent to the tail turret calorimeters to record fireball rise and growth and aircraft location with respect to time and the area viewed by the calorimeters. Filters were installed on the lenses for attenuation and spectral evaluation. Two of the cameras were located on the lower-body surface at Body Station 660 to record the locations and magnitudes of clouds below the aircraft. The remaining two cameras were mounted in the camera housing on the upper surface of the body approximately at Body Station 575, to scan the area above and forward of the aircraft. The field of view of these two cameras was coordinated with the views of the calorimeters for the crew compartment.

Two Traid Camera Corporation Automax 35-mm cameras (one main and one stand-by) were used to photograph an instrument panel located in the cockpit just aft of the pilot's seat. The photorecorder contained the following instruments: tail camera "on" lights; camera heater indicator;outside air temperature; airspeed; pressure altitude; bleed valve position (No. 6 engine); fuel flow (No. 6 engine); low speed rotor RPM (No. 6 engine); high speed rotor RPM (No. 6 engine); radar system target offset north-south coordinates (X_n); and radar system target offset east-west coordinates (X_e).

26

SECRET

Two Automax 35-mm cameras located above the upper surface of the wing on the centerline of the fuselage were used to record structural deflections (bending and torsion) of the wing and tail surfaces.

2.2.6 Oscillographs. Consolidated Engineering Corporation Model 5-119 oscillographs were installed as the major recording equipment. Eight oscillographs were mounted in racks in the forward crew compartment. Eleven oscillograph magazines were carried, eight installed and three carried as spares. Each magazine was loaded with 400 feet of thin photosensitive paper which provided ample running time for each oscillograph.

2.2.7 Time Coordination. Time coordination was provided for the oscillographs, photorecorder, deflection cameras, and the crew stations in the forward compartment.

Counters were operated at one-second intervals by an intervalometer and were photographed by the photorecorder, each deflection camera, and each oscillograph. The oscillographs also had a dynamic trace which marked the one- and ten-second intervals provided by the intervalometer.

The event signal (obtained by the test engineer pressing the event switch) was displayed by lights at all the stations and recorders except the oscillographs, where the event signal was marked by a shift in the base level of the dynamic trace.

A tuning-fork-controlled-time standard was used to provide correlation between the oscillographs for accurate time-base measurements.

In order to correlate data on the aircraft radar-scope camera, a counter was installed in the photorecorder to display the camera frame number.

2.3 INSTRUMENTATION CALIBRATION

In order to establish the relationship between the quantity measured and the deflection on the oscillograph, it was necessary to calibrate each channel. All transducers were originally calibrated by applying a series of accurately measured functions and recording the associated response on the oscillograph.

2.3.1 Radiometers and Calorimeters. The thermal-radiation-foil radiometers and disk calorimeters were designed, fabricated, and calibrated by NRDL. The calibration of the aircraft installation was accomplished by inserting accurately measured mv increments into the radiometer and calorimeter circuits to establish the galvan meter deflection per mv. The NRDL calibration, pre- and post-Redwing, established the relation between thermal radiation and mv readings.

The convective-cooling calorimeters were designed, fabricated, and calibrated by Boeing. The sensing element of the calorimeter was a thermocouple mounted on a small disk. Field calibrations were accomplished by accurately applying measured mv increments in series in the circuit before and after each flight. The Bureau of Standards data for mv output per degree Fahrenheit were used to obtain circuit references. The calorimeter-disk temperature was referenced to the ice point by immersing the reference junction of the circuit in a thermos of ice and water. The reference ice and water jugs were located in the forward crew compartment.

2.3.2 Thermocouples. All thermocouple circuits were calibrated electrically by the same method as the convective-cooling calorimeters. The thermocouple temperatures were also referenced to the ice point in the same manner as the convective-cooling calorimeters.

27

SECRET

2.3.3 Strain Gages. The point-load-calibration system, as described in Reference 19, was used to calibrate bending moment, shear- and torsion-combined-load circuits on the wing, fuselage, and stabilizer; and uncombined-moment bridges on the wing and stabilizer. A post-Redwing calibration was performed on the stabilizer-load circuits to extend the calibration range to be compatible with the magnitude of loads measured during Operation Redwing tests. All stress-bridge responses were calculated from the gage factors (ratio of change in resistance per unit strain).

At the time of the calibration of the strain-gage transducers, a precision resistor was momentarily shunted across one leg of each bridge. The bridge unbalance from the calibration load was then referenced to the unbalance from the resistor as a ratio. This unbalance-output ratio was constant, regardless of voltage or line-resistance changes. A resistor equivalent to the one used in calibration was included in the aircraft circuitry and used for ground and in-flight standardization.

2.3.4 Pressure Transducers. All pressure transducers were calibrated by applying manometer-measured pressure increments and recording their output. A resistor was momentarily shunted across one leg of the transducer bridge and a calibration ratio, which was constant regardless of voltage or line resistance, was obtained.

2.3.5 Accelerometers. The lateral and vertical accelerometers were calibrated in the laboratory by the use of an accurately controlled turntable. The accelerometers were mounted with their axis through the center of the turntable to measure centrifugal acceleration. The acceleration was adjusted by varying the speed of the turntable through the range that the particular element would be subjected. Angular accelerometers were calibrated by attaching them to a pivoted beam, the acceleration of which was controlled by a motor-driven cam at one end. Calibration ratios, similar to those obtained for strain-gage circuits, were obtained.

2.3.6 Control Surface Position Transducers. Calibration of the torsion-blade-positioning transducer, mounted on the hinge line of the control-surface element, was accomplished by moving the elevator, aileron, rudder, stabilizer or spoiler to a known series of position increments and recording the galvanometer deflection. This deflection was used as a ratio of the deflection caused by the standardizing resistor.

2.3.7 Deflection Cameras. Calibration was accomplished by photographing scale poles set at each target to establish the relationship between image displacement and actual deflection.

2.4 INSTRUMENT RELIABILITY

Every effort was made to utilize simple dc circuits for all electrical measurements. These circuits proved to be more reliable, as well as easier to maintain and set up, than circuits using vacuum-tube amplifiers and stepping switches.

A junction-box system was used in the aircraft-instrumentation wiring. Junction boxes were provided in the remote areas of the structure near anticipated transducer positions. These junction boxes were connected by shielded multi-conductor cables to a master junction box located above the forward wheel-well in the fuselage and from there to the recording equipment in the forward crew compartment.

Spare circuits were provided in anticipation of channel failure and new requirements.

They permitted growth and flexibility in instrumentation requirements without causing cables to be run through crowded structure areas. A system of short jumper cables in the master-junction box could be used to connect any transducer to any recording channel.

As indicated in Chapter 3, the reliability of the instrumentation was extremely high, in the order of 95 percent to 100 percent throughout the test program. Constant and considerable care was exercised in the protection of the instrumentation from moisture. Fabric rain-resistant covers were used to cover the entire left wing, the inboard section of the right wing, and both left and right stabilizers. These covers were kept on the aircraft, as allowed by maintenance and flight activities. In addition, the wing cavity surrounding the fuel cells, the aft unpressurized compartment and the horizontal-stabilizer cavities were ventilated with warm, dry, air during all possible time while the aircraft was on the ground. Two ground-blower units were used, each furnishing 1,200 ft^3/min of air at approximately 100 degrees Fahrenheit (dry-bulb temperature) with more than 60 percent of the ambient moisture removed. It is believed that the above noted precautions, in addition to the moisture proofing which was used on all strain-gage installations, accounted for the low percentage of instrumentation lost during the operation.

2.5 DATA REDUCTION AND HANDLING

The magnitude of data obtained at the test site was so great that, with the time and manpower available, only a small percentage was actually reduced. Prior to each participation, a list of all required data was prepared and priority assigned for reduction purposes.

Immediately after the aircraft landed from a shot participation, all oscillograph and camera magazines were removed and the records were processed by the Flight Test Instrumentation Group (Figure A.1, Appendix A). Each channel of the oscillographic data and camera information was inspected by the Instrumentation Group for possible malfunction or complete failure before the records were turned over to the Flight Test Operations Group for data reduction. All field-data reduction was accomplished manually. The reduced data consisted primarily of maximum values obtained per channel with the associated time relative to time zero. Certain channels, however, required complete reduction into time-history plots. The reduced data were furnished to the Positioning and Stress Groups for analysis and correlation with predicted-energy inputs and aircraft response.

Upon return to the United States, all recorded data were scanned and interpreted by the Boeing Flight Test Operations and Instrumentation Groups in preparation for reading and processing by the Data Processing Group through a semi-automatic data-reduction system. The reduced data were furnished as time histories to the Special Studies Stress Group for analysis. The measured results presented in Chapter 3 were obtained from the final reduced data. The time-history data is presented in its entirety in Reference 23.

Data reduction began with the identification of traces on the oscillograms and the marking of the time coordinates; time of detonation, or time zero; and time of gust arrival at the aircraft. Zero references were also established. Each trace was then read with a Telereader which was equipped with a set of cross hairs for measuring trace displacement and distance along the time axis. The Telereader measurements were in arbitrary-reader units and were fed through a Telecordex unit into an IBM-summary punch which transferred the information to IBM cards. The Telecordex also supplied additional information for the processing of the data. The IBM cards, together

SECRET

with data reduction program cards, were inserted into an IBM type 701 computer which calculated the data and recorded the answers as IBM punch cards, from which a data tabulation was obtained. IBM type 650 and Burroughs type E-101 computers were also used for processing minor portions of the data. Plotting of the final reduced data was accomplished with an automatic electronic Teleplotter using the final data cards from the computers. The plotted points were faired manually so that the resultant curves were corrected time-history representations of the oscillogram traces.

SECRET

Chapter 3

RESULTS

The results presented in this chapter are based on final reduction of the data from Operation Redwing. Brief descriptions of the shot participations are given in the following subsections. Tabulations of shot information, aircraft positions, energy inputs, and aircraft responses are presented in Tables 3.1 through 3.9. These tables afford a general comparison of predicted results with measured values. Also included are representative time histories of various weapon effects and aircraft responses (Figures 3.1 through 3.5).

A complete presentation of the final reduced data of Operation Redwing appears in Reference 23. Analysis and correlation of the data with theoretical values will appear in WADC TR 57-?13, to be published in the near future.

3.1 SHOT CHEROKEE

Shot Cherokee was detonated in the vicinity of Site Charlie, Bikini Atoll, near dawn on 21 May 1956. The device was dropped by a B-52 aircraft from an altitude of 40,000 feet to a burst altitude of 4,300 feet. The best available data indicates the device yield was 3.8 Mt. Because of an error, the device was detonated approximately 21 seconds before the assigned time zero. The detonation occurred approximately 20,000 feet northeast of the desired ground zero.

The B-52 effects aircraft at time zero was not out of the turn which was to have put the aircraft tail-on at the assigned time zero. As a result, the aircraft received partial side-on thermal and shock input rather than the desired tail-on input. Relative to the actual detonation point, the aircraft was within 1,800 feet of the desired horizontal range at time zero and 3,300 feet at shock-arrival time.

Based on the yield and aircraft location, the radiant exposure was approximately 74 percent of that which would have been predicted. The overpressure and material velocity were approximately 10 percent higher than would have been predicted. The peak thin-skin temperature was 48 percent of the limit temperature. Measured overpressure was 59 percent of limit. Approximately 50 percent of the allowable limit wing-bending moment was recorded at Wing Station 444. The horizontal tail received approximately 51 percent of the allowable limit bending moment at Stabilizer Station 300. In this shot the load measurements on the right side of the stabilizer exceeded those on the left side. No instrumentation was provided for measurement of bending moment at Stabilizer Station 300 on the right side. However, there was a provision for measuring the bending moment at Stabilizer Station 56 on both sides. The maximum Stabilizer Station 300 bending moment was computed by multiplying the left Stabilizer Station 300 moment by the ratio of the right-to-left Stabilizer Station 56 bending moments. Table 3.8 indicates on which shots this procedure was used.

Aircraft damage was confined to thermal damage on secondary items and consisted of the following: (1) burning, to the point of separation, of the left-hand aileron-control-tab seal; (2) scorching of the right-hand aileron-control-tab seal; (3) blistering of paint on a small area of 0.032-magnesium skin just aft of the wing rear spar behind No. 4

31
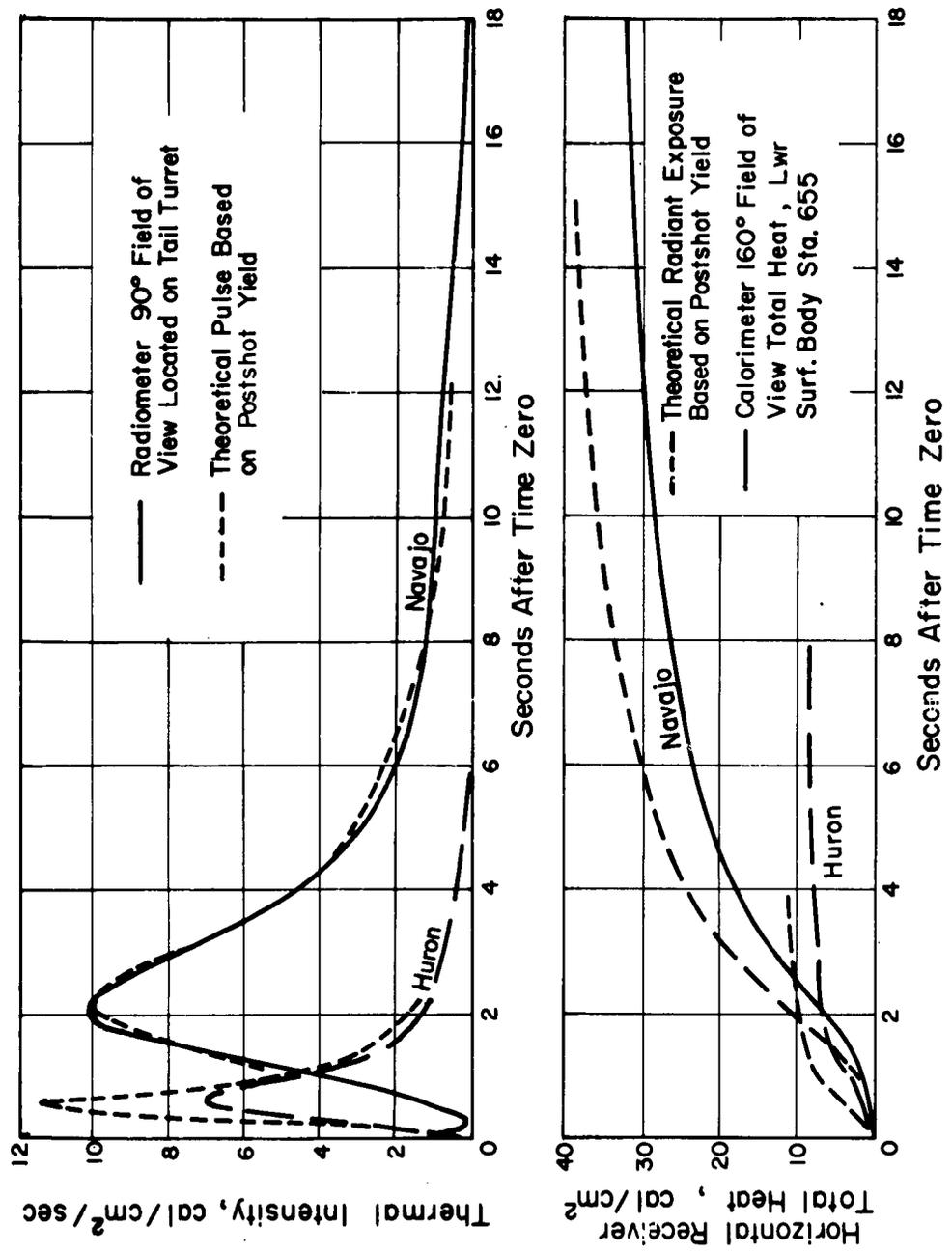
Figure 3.1 Typical radiometer and calorimeter measurements.

32
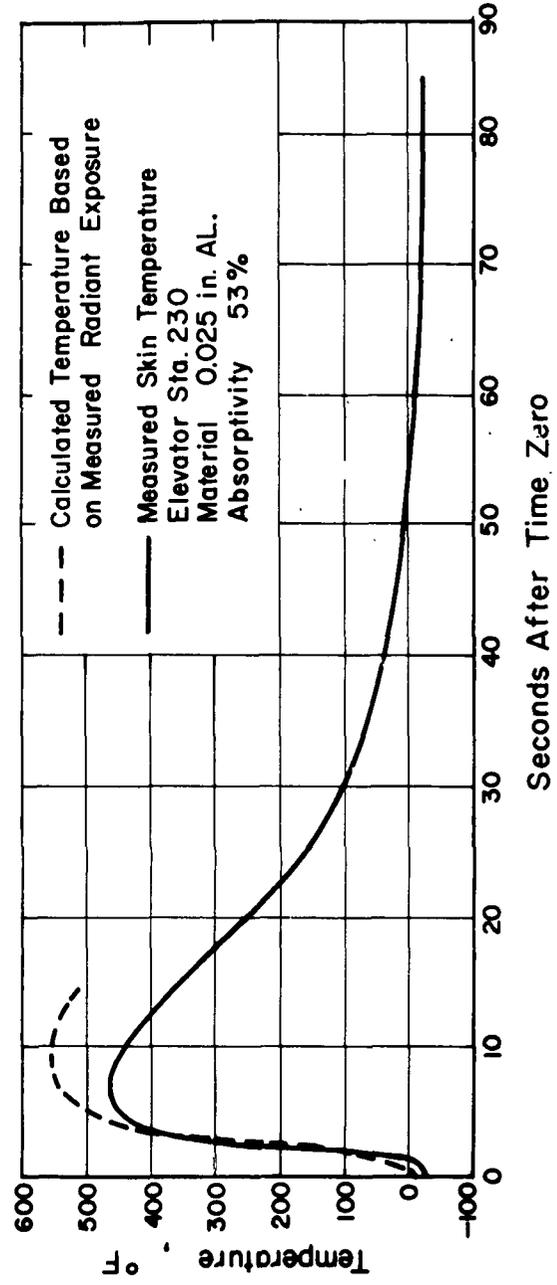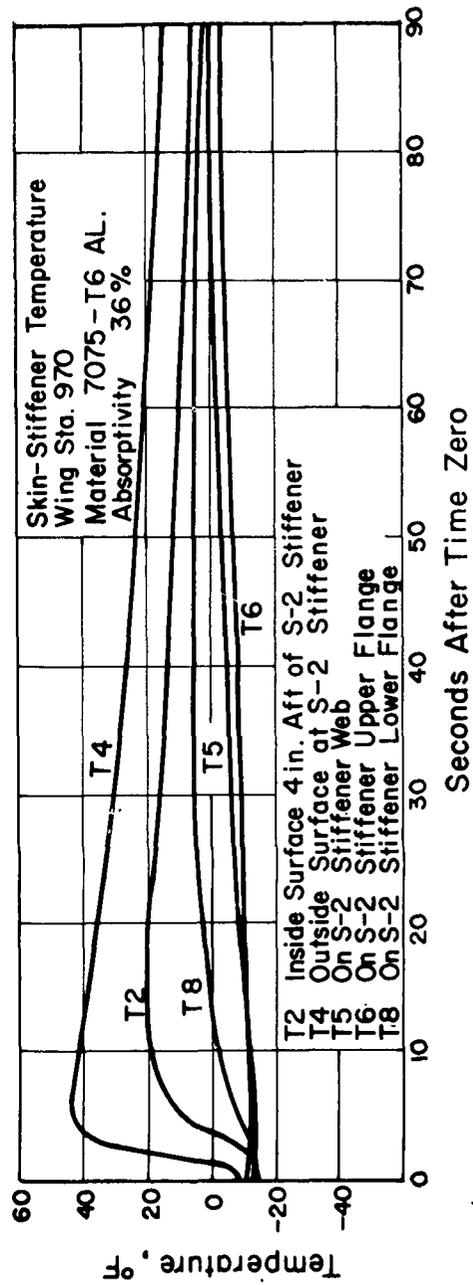
Figure 3.2 Typical measured wing and tail temperature response, Shot Navajo.

33

SECRET
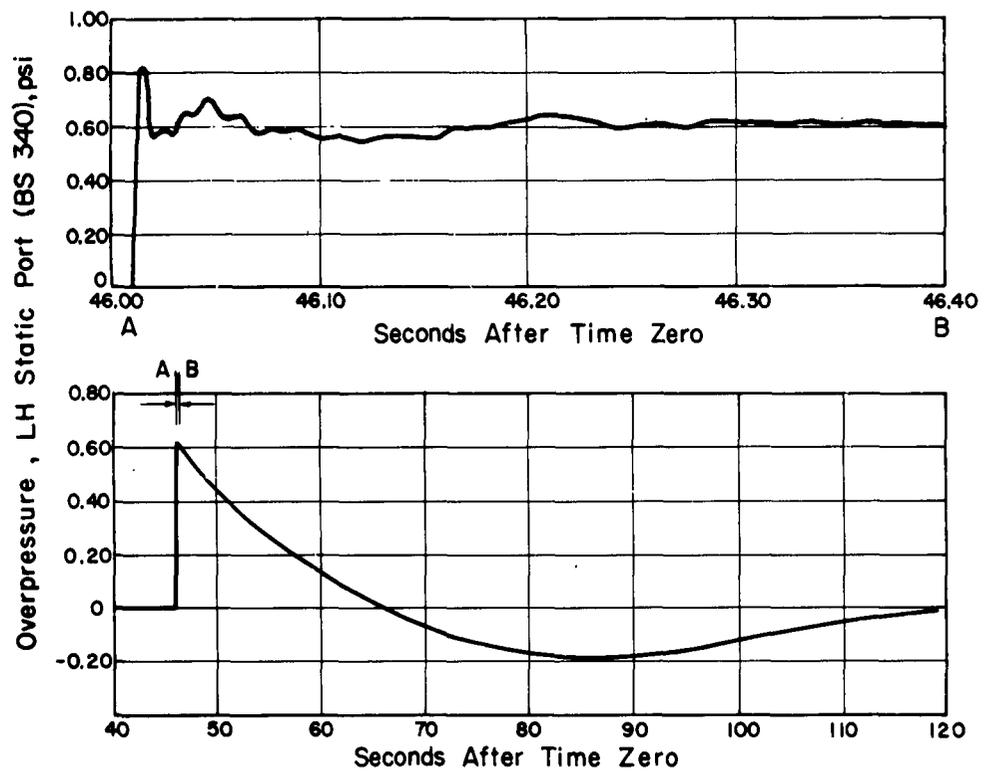
Figure 3.3 Typical overpressure measurement, Shot Navajo.
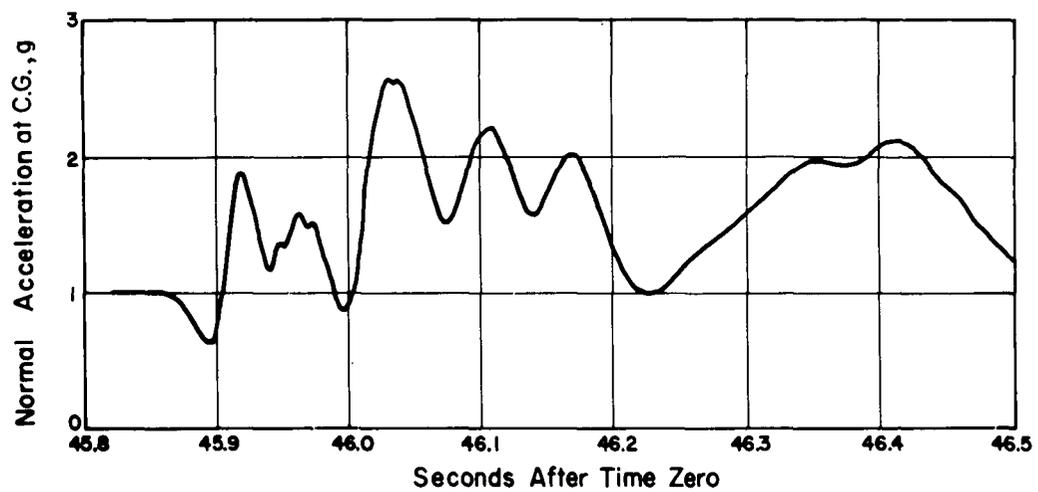
Figure 3.4 Typical aircraft center of gravity acceleration, Shot Navajo.

34

SECRET

nacelle; (4) scorching of small scattered areas on the bomb-bay door and stabilizer-fuselage seals; and (5) burning of the unpainted rain-erosion coating on the right-hand side of the rudder-trailing edge as a result of the partial side-on exposure.

Three hundred and thirty-four channels of instrumentation, 97 percent of which operated successfully, were recorded.

3.2 SHOT ZUNI

Shot Zuni was detonated at Site Tare, Bikini Atoll, near dawn on 28 May 1956. The device yield was approximately 3.5 Mt.

Based on yield and aircraft location, the radiant exposure was approximately 115 percent of that which would have been predicted. The measured overpressure was in agreement with that which would have been predicted. The thermal response of the structure was considerably lower than anticipated. The maximum thin-skin tempera-

TABLE 3.1 SHOT INFORMATION

Shot Name	Yield			
	Positioning (Preshot)	Nominal (Preshot)		Official Preliminary (Postshot)
	Mt	Mt		Mt
Cherokee	6.0	4.0	−5.0	3.8
Zuni	5.0	1.0	−3.0	3.5
Dakota	0.85	0.8	—	1.15
Mohawk	0.7	0.3	−0.4	0.35
Apache	5.0	2.0	−3.0	1.9
Navajo	10.0	6.0	−8.0	4.8
Tewa	15.0	6.0	−8.0	5.0
Huron	0.3	0.20	−0.25	0.27

ture recorded was 63 percent of limit in a black-painted, 0.051-magnesium hydraulic-pack access door located on the left-outboard wing. The elevator tab seals and small section of the bomb-bay door and stabilizer-fuselage seals were slightly scorched. The black paint on a small test area on the lower surface of the ECM radome was blistered, and the gray paint on a small test panel on the lower surface of the left-hand wing was partially peeled. The aircraft received 69 percent of the basic airplane-limit allowable on the wing and 59 percent on the horizontal stabilizer.

Three hundred and thirty-four channels of instrumentation, 97 percent of which operated successfully, were recorded during the flight.

3.3 SHOT FLATHEAD

Shot Flathead was detonated on a barge off Site Dog, Bikini Atoll, near dawn on 12 June 1956. Because of bombing-navigation-system difficulties, the aircraft was forced to abort the Shot Flathead mission. No measurable inputs or responses were obtained.

SECRET

TABLE 3.2   AIRCRAFT LOCATION RELATIVE TO GROUND ZERO AT TIME ZERO

Shot	Horizontal Range *	Absolute Altitude	Orientation Off Tail-On	True Airspeed †	Center of Gravity Location	Gross Weight
	kilofeet	kilofeet	deg	ft/sec	pct MAC	kip
Cherokee						
Assigned	34.0	31.0	0	772	26.0	273.0
Measured	35.8	31.0	33 R	733	26.9	277.0
Zuni						
Assigned	20.0	32.0	0	772	26.0	274.0
Measured	23.8	32.0	15 L	776	25.9	273.0
Dakota						
Assigned	12.0 ‡	22.0	0	772	26.0	275.0
Measured	11.5	22.0	3 L	786	25.5	271.7
Mohawk						
Assigned	7.5 ‡	25.0	0	772	26.0	275.0
Measured	8.2	25.0	0	784	27.5	280.5
Apache						
Assigned	15.0 ‡	34.0	0	772	26.0	277.0
Measured	18.6	34.0	9 L	754	26.8	270.6
Navajo						
Assigned	19.0 ‡	38.0	0	772	26.0	273.5
Measured	18.3	38.0	2 R	768	27.2	275.3
Tewa						
Assigned	28.5 ‡	41.0	0	772	26.0	274.5
Measured	26.7	41.0	4 R	769	26.8	273.9
Huron						
Assigned	6.5 ‡	20.0	0	772	26.0	273.0
Measured	5.7	20.0	6 L	757	26.8	266.4

* Horizontal ranges obtained from BNS.

† Measured airspeeds are determined from the aircraft airspeed indicator and atmospheric data presented in Table C.1.

‡ Aircraft positioned for shock arrival location.   Time zero values based on no wind.

36

SECRET

3.4 SHOT DAKOTA

Shot Dakota was detonated on a barge off Site Dog, Bikini Atoll, near dawn on 26 June 1956. The device yield was approximately 1.15 Mt. This was greater than the positioning yield.

The aircraft was positioned to receive approximately 90 percent of the basic airplane-allowable-limit overpressure, in order to check the possibility of flap criticality under this type of loading.

Based on the yield and aircraft location, the radiant exposure was 81 percent and overpressure 98 percent of that which would have been predicted. The maximum thin-
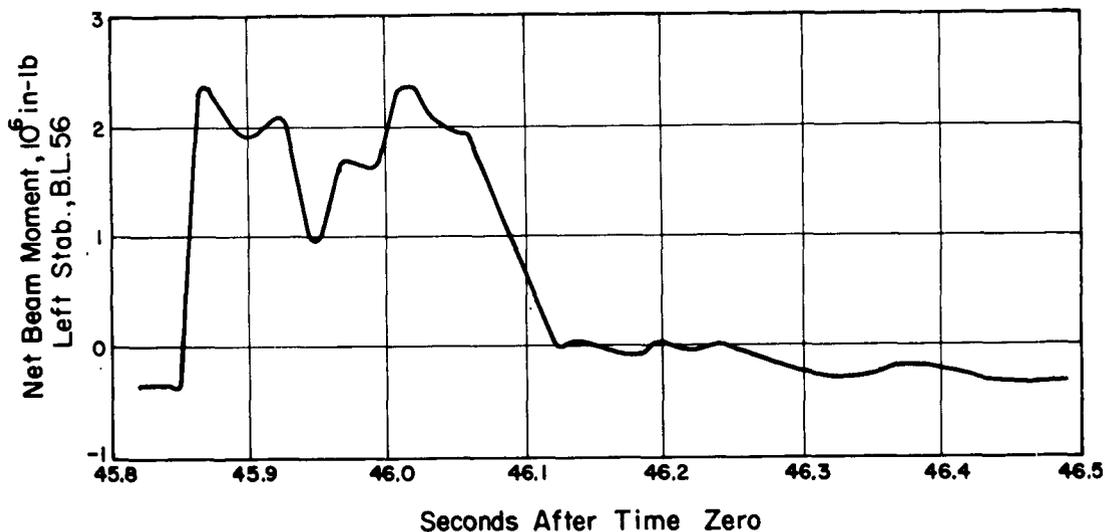
Figure 3.5 Typical horizontal stabilizer moment response, Shot Navajo.

skin temperature recorded was 101 percent of limit on a black-painted panel at Body Station 1141. The overpressure recorded was 110 percent of the basic-airplane-limit allowable. An examination of the flaps, both from the exterior and through a number of the closure-access holes on the top of the flaps, showed no evidence of permanent set or other damage to the flap ribs, spars, or surfaces. Sixty-two percent of the allowable-limit wing-bending moment was recorded at Wing Station 444. The horizontal tail received 100 percent of the limit-allowable bending moment at Stabilizer Station 300.

Examination of the aircraft revealed the following minor damage: (1) scorching of aileron-control-tab seals, wing-flap-pile seals attached to the lower-wing-trailing-edge structure, bomb-bay door seals, stabilizer-body seals, filler material at the intersection of vent openings and the lower surface of the fuselage at Body Station 1140, and black paint on small test areas on the ECM radome, fuselage, wheel-well-door fairing, elevator, and wing-trailing-edge access door; (2) slight bearing failure of the edge of the fuselage skin surrounding the forward wheel-well resulting from overpressure on the wheel-well door forcing the edge of the door skin against the edge of the fuselage skin; (3) pinching, to the point of separation, of the forward wheel-well door-rubber seal; (4) bond failure between skin and stiffeners on the black-painted hydraulic-pack access door on the left-hand wing at Wing Station 1035 (Temptape readings on the access door showed that a temperature in excess of 500 degrees Fahrenheit was reached. The thermocouple circuit for this location malfunctioned during this test.); and (5) burning of the black-painted metal sun shades on the lower end of the optical bombsight, because

37

TABLE 3.3 AIRCRAFT LOCATION RELATIVE TO GROUND ZERO AT TIME OF SHOCK ARRIVAL

Shot	Gust Arrival Time	Horizontal Range	Absolute Altitude	Orientation Off Tail-On	True Airspeed	
					Pregust *	Postgust † ‡
	sec	kilofeet	kilofeet	deg	ft/sec	ft/sec
Cherokee						
Assigned	70.5	88.5 §	31.0	0	772	707
Measured	68.1	85.2	31.0	11 R	766	704
Zuni						
Assigned	45.2	54.4 §	32.0	0	772	681
Measured	51.8	62.4	32.0	6 L	776	706
Dakota						
Assigned	31.0	35.9	22.0	0	772	705
Measured	28.0	32.7	22.0	2 L	791	713
Mohawk						
Assigned	29.1	30.0	25.0	0	772	710
Measured	32.0	33.4	25.0	0	790	742
Apache						
Assigned	40.6	46.3	34.0	0	772	672
Measured	48.6	53.8	34.0	1 L	772	707
Navajo						
Assigned	46.0	54.5	38.0	0	772	658
Measured	45.8	53.3	38.0	0	762	672
Tewa						
Assigned	62.0	76.4	41.0	0	772	658
Measured	72.4	81.1	41.0	2 R	756	680
Huron						
Assigned	23	24.3	20.0	0	772	717
Measured	23.3	23.2	20.0	1 L	766	710

* Measured airspeeds are determined from the aircraft airspeed indicator and atmospheric data presented in Table C.1.

† Airspeed immediately after shock arrival.

‡ Measured airspeeds are computed from measured incremental pressure data and preshock airspeeds.

§ Aircraft positioned for time-zero location. Values are based on no wind.

TABLE 3.4 THERMAL INPUT

Shot	Calorimeters					Radiometers	
	Tail Turret Aimed at Ground Zero, Bandpass 0.2 to 4.0 μ		Body Station 655 Aimed Vertically Down, Bandpass 0.2 to 4.0 μ		Forward Cabin Outside, 48 deg UP Aimed Forward, Bandpass 0.2 to 4.0 μ	Tail Turret Aimed at Ground Zero, Time to Second Maximum	
	160 deg Field View	90 deg Field View	160 deg Field View		90 deg Field View		
	Measured*	Avg of Three Measurements*	Predicted†	Avg of Two Measurements‡	Measured	Predicted†	Avg of Two Measurements
	cal/cm²	cal/cm²	cal/cm²	cal/cm²	cal/cm²	sec	sec
Cherokee	36.3	34.6	31.5	23.2	0.165	1.95	1.94
Zuni	36.6	34.9	25.3	29.0	0.125	1.87	1.89
Dakota	28.6	28.6	26.9	21.9	0.135	1.07	1.10
Mohawk	13.1	9.0	11.3	9.5	3.7	0.59	0.68
Apache	14.2	15.6	18.4	11.8	0.025	1.38	1.41
Navajo	39.2	41.9	39.2	33.7	0.050	2.19	2.15
Tewa	20.7	21.5	27.1	16.3	0.030	2.24	2.09
Huron	8.4	8.2	11.4	7.7	0.060	0.52	0.60

* Readings corrected to direct line of sight.
† Based on postshot yield and actual aircraft location.
‡ Readings corrected to true vertical.

the clamshell doors were not closed at time zero.

A total of three hundred and twenty eight channels of instrumentation, 98 percent of which operated satisfactorily, were recorded.

3.5 SHOT MOHAWK

Shot Mohawk was detonated at Site Ruby, Eniwetok Atoll, near dawn on 3 July 1956. The device yield was approximately 0.35 Mt.

Based on the yield and aircraft location, the radiant exposure was 84 percent and overpressure 92 percent of that which would have been predicted. The maximum thin-

TABLE 3.5 OVERPRESSURE AND GUST INPUTS

| Shot * | Gust | | | Overpressure |
	Shock Front Velocity	Shock Impingement Angle †	Material Velocity	Avg. of 9 Transducers Fus. and Stab.
	ft/sec	deg	ft/sec	psi
Cherokee				
Predicted	1,068	24.2	71	0.43
Measured	1,066	26.9	74	0.47
Zuni				
Predicted	1,077	30.0	92	0.55
Measured	1,072	33.5	89	0.55
Dakota				
Predicted	1,124	35.2	101	0.90
Measured	1,118	37.2	98	0.88
Mohawk				
Predicted	1,088	38.4	63	0.48
Measured	1,087	38.5	56	0.44
Apache				
Predicted	1,063	35.2	83	0.45
Measured	1,053	34.9	77	0.44
Navajo				
Predicted	1,071	38.4	120	0.57
Measured	1,057	42.2	121	0.61
Tewa				
Predicted	1,035	31.0	88	0.35
Measured	1,014	28.1	84	0.36
Huron				
Predicted	1,115	41.6	75	0.70
Measured	1,113	40.0	67	0.64

* Predicted values based on postshot yields.
† Angle from horizontal.

skin temperature recorded at Body Station 1141 was 55 percent of limit. The aircraft received 55 percent of the allowable-limit overpressure, 61 percent of the allowable-limit-bending moment at Wing Station 444, and 63 percent of the allowable-limit-bending moment at Stabilizer Station 300.

Solid-cloud conditions existed from an altitude of 1,600 feet up to approximately 30,000 feet. Shortly after time zero, moderate-rime icing was reported to exist at 15,000 feet. The cloud conditions produced a high reflectance as indicated by data obtained from a calorimeter located on the nose of the aircraft just forward of the cockpit windows. The oscillograph trace recording the radiant intensity went off the paper; however, using the curve shape from previous shots, it was estimated that approximately 3.72 cal/cm^2 were received at this location. A 160-degree field-of-view calorimeter located in the tail turret looking at ground zero received 13.1 cal/cm^2. As a result of the reflected energy, rain-erosion coatings on the upper-nose radome, the

TABLE 3.6   THERMAL RESPONSE DATA

Shot	Wing Station 1032, 0.032 Mg			Body Station 640, 0.032 Mg		
	Absorptivity*	Temperature Rise†	Total Temperature†	Absorptivity*	Temperature Rise†	Total Temperature†
	pct	F	F	pct	F	F
Cherokee						
Predicted	23	188	200	21	178	190
Measured	23	‡	‡	21	131	150
Zuni						
Predicted	25	248	262	20	207	221
Measured	25	73	89	20	137	166
Dakota						
Predicted	35	268	318	23	184	234
Measured	35	159	209	23	191	244
Mohawk						
Predicted	40	155	200	30	120	165
Measured	40	101	143	30	108	150
Apache						
Predicted	27	117	119	32	145	147
Measured	27	46	53	32	128	134
Navajo						
Predicted	28	323	307	33	402	386
Measured	28	128	120	33	298	285
Tewa						
Predicted	31	177	144	22	131	99
Measured	31	106	86	22	65	35
Huron						
Predicted	42	133	193	23	75	135
Measured	42	58	122	23	66	118

* Measured value obtained from measurements with the Boeing reflectometer.
† Predicted values based on measured inputs.
‡ Instrumentation malfunction.

41

SECRET

TABLE 3.7 THERMAL RESPONSE DATA

All absorptivities greater than 30 percent represent test panels.

Shot	Body Station 1150, 0.032 Mg			Elevator Station 230, 0.025 Al		
	Absorptivity*	Temperature Rise†	Total Temperature†	Absorptivity*	Temperature Rise†	Total Temperature†
	pct	F	F	pct	F	F
Cherokee						
Predicted	25	219	231	35	273	285
Measured	25	105	142	35	177	177
Zuni						
Predicted	24	246	260	53	498	512
Measured	24	136	166	53	325	335
Dakota						
Predicted	87	739	789	83	662	712
Measured	87	545	607	83	512	545
Mohawk						
Predicted	92	370	415	90	320	365
Measured	92	275	330	90	277	302
Apache						
Predicted	25	116	118	50	213	214
Measured	25	58	80	50	215	205
Navajo						
Predicted	24	299	283	53	573	557
Measured	24	150	155	53	493	463
Tewa						
Predicted	28	172	140	42	286	256
Measured	28	‡	‡	42	185	150
Huron						
Predicted	28	94	153	54	154	214
Measured	28	65	135	54	98	138

* Values obtained from measurements with the Boeing reflectometer.
† Predicted values based on measured inputs.
‡ Instrumentation malfunction.

42

SECRET

TABLE 3.8 AIRCRAFT PRIMARY STRUCTURE GUST RESPONSE

Shot	Load Ratios						
	Wing		Horizontal Stabilizer				Fuselage
	Moment Wing Station 407 - 500		Moment Stabilizer Station 300		Total Tail Load		Shear Body Station 1332
	Predicted*	Measured	Left Hand (Measured)	Right Hand †	Predicted*	Measured	Measured
	pct‡	pct‡	pct‡	pct‡	pct‡	pct‡	pct§
Cherokee	64	52	38	51	38	20	31
Zuni	77	60	59	54	57	35	33
Dakota	77	62	100	100	98	60	45
Mohawk	62	61	47	63	50	27	34
Apache	62	59	46	60	48	28	30
Navajo	80	82	85	99	82	52	43
Tewa	57	52	33	33	32	19	—
Huron	67	55	71	69	71	45	—

* Predicted values based on measured inputs and adjusted $K_g D$ factors (See Sections 4.7 and 4.8).
† Right stabilizer moment calculated from left stabilizer measured moment using ratio of left to right stabilizer moments at Buttock Line 56 (See Section 4.5).
‡ Percent of limit allowable.
§ Percent of front-gear-first-landing design limit load (Reference 21, page 2B-3).

TABLE 3.9 AIRCRAFT MAXIMUM MEASURED VERTICAL ACCELERATION

Shot	Vertical Acceleration, g									
	Aircraft Center of Gravity	Aft Fuselage BS 1655	Inboard Nacelle Equipment Bay WS 531		Outboard Nacelle Equipment Bay WS 915		External Tank Equipment Bay WS 1155		WS 1345	
			LH	RH	LH	RH	LH	RH	LH	RH
Cherokee	1.95	3.21	2.46	2.79	3.60	4.20	5.40	4.85	*	6.00
Zuni	2.34	4.54	3.21	^.95	4.96	5.50	6.34	6.90	*	8.30
Dakota	2.76	6.63	4.00	3.70	*	7.00	7.35	6.90	12.20	*
Mohawk	2.02	3.97	2.65	2.53	*	4.90	6.23	5.55	*	*
Apache	2.17	3.78	2.87	2.83	*	4.80	7.00	6.10	*	*
Navajo	2.56	5.70	3.26	3.40	*	6.10	7.47	7.57	*	*
Tewa	1.91	2.90	2.53	2.46	*	*	5.17	4.60	5.60	*
Huron	2.18	5.32	3.10	3.11	*	*	6.60	7.00	8.40	*

* Instrumentation malfunction.

43

glide-path antenna cover, the upper side of the plastic wing tips, and the fin tip were blistered. At the time the aircraft landed, approximately 90 percent of the rain-erosion coating on the upper-nose radome was gone. The temperature on the top of the elevator tab (unpainted Al) reached 157 degrees Fahrenheit, whereas the temperature on the lower side (Vita-Var-painted Al) reached 96 degrees Fahrenheit.

Examination of the aircraft revealed the following additional minor damage: (1) scorching of the pneumatic-duct cover in the left- and right-wing trailing edge at Wing Station 845 over a length of approximately 8 inches (the radiation reached the duct cover through a small gap between the wing-trailing-edge structure and the leading edge of the flap); and (2) burning of the crew-compartment-curtain-draw cords on the ends where they were knotted on the upper-forward side of the curtains at the grommet locations (the crew reported some smoke in the crew compartment as a result).

Three hundred and twenty-three channels of instrumentation, 97 percent of which operated successfully, were recorded.

3.6 SHOT APACHE

Shot Apache was detonated near dawn on a barge off Site Flora, Eniwetok Atoll, on 9 July 1956. The device yield was approximately 1.9 Mt.

Based on the yield and aircraft location, the thermal input received was 64 percent and overpressure 98 percent of that which would have been predicted. The maximum thin-skin temperature recorded was 34 percent of limit at Elevator Station 230. The measured absorptivity at this station was 0.50. The overpressure recorded was 55 percent of the airplane-limit allowable. Fifty-nine percent of the allowable-limit-wing-bending moment and 60 percent of the horizontal-tail-allowable-limit-bending moment was recorded. The aircraft received no visible damage, except for slight scorching of the bomb-bay-door seals and aileron-tab seals.

Three hundred and sixteen channels of instrumentation, 97 percent of which operated satisfactorily, were recorded.

3.7 SHOT NAVAJO

Shot Navajo was detonated on a barge off Site Dog, Bikini Atoll, near dawn on 11 July 1956. The device yield was approximately 4.8 Mt.

Based on the yield and the actual-aircraft position, the radiant exposure was 86 percent of the value which would have been predicted, and the overpressure was 107 percent of that which would have been predicted. The maximum thin-skin temperature recorded was 77 percent of limit on a gray-painted panel. The measured overpressure was 76 percent of the allowable limit. The wing received 82 percent of the allowable-limit moment at Wing Station 444. In terms of allowable-bending moment, the left stabilizer was critical at Stabilizer Station 300 with a response of 85 percent of the allowable limit. The right stabilizer had no instrumentation at this station. However, using the ratio of right to left stabilizer loads at Buttock Line 56, the right stabilizer moment at Stabilizer Station 300 was estimated to have reached approximately 99 percent of the allowable limit.

The damage incurred included: (1) scorching and burning of aileron-control-tab seals, flap-leading-edge-pile seals, bomb-bay-door seals, fuselage-stabilizer seals, and the felt padding on the bottom of the bomb-bay-door-shoring beam; and (2) light skin buckling in local areas where paint had chipped or eroded off the wing-trailing edge aft of No. 7 engine and on the lower-cowl skins on Engines 1, 5, and 6. The zinc-chromate primer was scorched on the inside of the cowl skins at these local areas.

44

SECRET

Figure 3.7 Damage photo, ECM radome, Shot Huron.

Figure 3.6 Damage photo, bomb-bay door, Shot Huron.

45

SECRET

In addition to the thermal damage, the left forward-gear landing light was broken. Glass found in the fuselage cavity indicated that the damage occurred while the gear was in the r .tracted position and may have been a result of structural deflection caused by the overpressure and gust.

Three hundred and twenty-seven channels of instrumentation, 98 percent of which recorded satisfactorily, were recorded during this shot.

3.8 SHOT TEWA

Shot Tewa was detonated near dawn on 21 July 1956, on a barge approximately midway between Sites Charlie and Dog in the Bikini Atoll. The device yield was approximately 5.0 Mt.

Based on the yield and actual-aircraft location, the radiant exposure was 60 percent of that which would have been predicted, and the overpressure was 103 percent of that which would have been predicted. The maximum thin-skin temperature recorded was 25 percent of limit. The measured overpressure was 45 percent of the allowable limit, and the wing received 52 percent of the allowable-limit moment at the critical Wing Station 444.

The left and right stabilizer-measured loads were in close agreement on this shot and received 33 percent of the allowable-limit moment at Stabilizer Station 300.

The bomb-bay doors and ECM radome were unshored for this shot. At the time the shoring was removed from the radome, the ECM cavity was vented and sealed in a manner simulating the production aircraft. The measured overpre.'sure was equal to the estimated-allowable ultimate for the radome. No failure or permanent set occurred in either component.

There was no evidence of aircraft damage, either from radiant energy, overpressure, or gust.

Three hundred and thirty-four channels of instrumentation, 98 percent of which recorded satisfactorily, were recorded.

3.9 SHOT HURON

Shot Huron was detonated near dawn on 22 July 1956, off Site Gene in the Eniwetok Atoll. The device yield was approximately 0.27 Mt. Based on the yield and actual-aircraft location, the radiant exposure was 68 percent and overpressure 91 percent of that which would have been predicted.

The maximum thin-skin temperature response was only 22 percent of limit. The overpressure experienced was 80 percent of the allowable limit, bending moment at Wing Station 444 was 55 percent of the allowable limit, and 71 percent of the allowable-limit moment was developed at Stabilizer Station 300.

The ECM radome and bomb-bay doors were unshored for this shot as they were for Shot Tewa. The radome suffered a complete failure as a result of the overpressure (Figure 3.7). The forward panel of the lower aft left-hand bomb-bay door was buckled over approximately a two-foot length. There was visual evidence of damage to one door rib and probable damage to a second rib in this location. Also, slight permanent skin buckles occurred on the lower-left-forward door adjacent to the hinge support (Figure 3.6). No other damage was noted.

Three hundred and thirty-one channels of instrumentation, 99 percent of which recorded satisfactorily, were recorded.

46

SECRET

Chapter 4
DISCUSSION

In general, the aircraft responses desired were in the range of 80-to-100 percent of the allowable limits, because larger responses can be more accurately measured, and because extrapolation to determine maximum capability would be minimized. Modifications to the original positioning plans resulted when positioning yields and shot sequences were revised both prior to, and after arrival at, the Eniwetok Proving Ground (EPG); and field-data reduction and preliminary correlation from shots already fired indicated the desirability of revising the aircraft's positions for subsequent shots.

4.1 INSTRUMENTATION

The instrumentation used in Operation Redwing was, in general, adequate, reliable, and produced the data necessary for a successful participation in the test series. The functional reliability of the instrumentation was high throughout the test program and was at least 95 percent effective. Environmental conditions for the instrumentation on Operation Redwing were severe with regard to temperature and humidity. The high degree of reliability in this adverse environment may be largely attributed to the moisture-proofing and the dehumidifying blowers which circulated warm, dry air over the instrumentation during the time that the aircraft was on the ground.

Every effort was made to utilize simple dc circuits for all electrical components of the measurement systems. Combined strain-gage circuits provided a convenient method for obtaining flight loads. However, some difficulty in maintenance was experienced since failures in the various components of the combined circuits were not easily detected. Spare load-measuring circuits were utilized when the primary circuitry malfunctioned, although extensive use of the secondary instrumentation was not necessary. Bakelite strain gages showed a considerably higher degree of durability than the paper-backed type.

Structural-load-measuring instrumentation was monitored for repeatability by controlled flight maneuvers throughout the field-test period, and the responses were compared to data obtained in similar maneuvers prior to the departure of the aircraft for the EPG.

The horizontal-stabilizer-loads-instrumentation checks showed the responses to be consistent throughout the test program for the range of loads for which the strain gages were originally calibrated. However, loads measured during Operation Redwing were as much as three times as great as the loads applied during the original strain-gage calibration. It was recognized that the extrapolation of the calibration data into the range of measured loads could result in significant error. Since the horizontal tail appeared to be the limiting factor in the aircraft capability for nuclear-weapon effects, it was considered mandatory to recalibrate the loads instrumentation into the high-load range. In general, the posttest calibration showed that the extrapolation from the original calibration data was not greatly in error, but final test data were transcribed on the basis of the revised calibration.

In reviewing the temperature-measuring-thermocouple installations during the cor-

47

relation work subsequent to Operation Redwing, it was noted that moisture-proofing had been applied over most of the thermocouples and their adjacent leads. The quantity of sealant material used is not known since the aircraft was delivered to a depot for removal of instrumentation, maintenance, and repair prior to an evaluation of the installations. Preliminary evaluation tests indicate that a considerable heat-sink effect may be caused by a heavy coating of sealant. This effect is discussed in more detail in Section 4.4.

Thermocouple circuits were susceptible to failures in high-vibration areas, especially where water, fuel, or hydraulic fluid was present. The contaminants tended to saturate the leads, loosen the waterproofing, and sometimes cause the thermocouples to open or corrode.

The calorimeters and radiometers proved to be reliable in their operation, but some maintenance problems resulted from cracked filters.

Accelerometers proved to be susceptible to malfunctions or failures apparently arising from local vibration and environmental temperature.

Pressure transducers also suffered from the effects of structural-support vibration and from moisture, which was almost impossible to avoid because of condensation in the ports and bellows.

The accuracy of the data obtained in Operation Redwing is too diverse in scope to be dealt with in a general way. Accuracy is dependent upon the type of input being measured; the technical limitations of equipment currently available for measuring such input; and other factors such as the installation conditions, signal transmission, recording equipment, and the methods used to transcribe the data. For these reasons the data accuracy is stated in terms of probable error on each of the individual data plots which appear in Reference 23.

4.2 NUCLEAR RADIATION

Nuclear radiation was found to be insignificant for the B-52 locations relative to the burst points for Operation Redwing. This is based on theoretical considerations, film badges worn by the flight crew, and dosimeter readings taken on the aircraft after landing.

4.3 THERMAL EXPOSURE

Two calorimeters were mounted on the lower surface of the fuselage as primary instruments to record total thermal energy received on a horizontal surface. These instruments were the 160-degree-field-of-view type. Thermal inputs predicted for a horizontal surface were more than the measured exposures from the 160-degree-field-of-view calorimeters for all shots except Shot Zuni, as shown in Table 3.4. During Shot Zuni, the measured-radiant exposure to the horizontal surface was approximately 15 percent higher than predicted. The predicted values were based on the postshot yields and aircraft locations. A review of the motion pictures taken from the tail cameras indicates little evidence of atmospheric clouds which could be considered to have any significant attenuating effect on the thermal exposure except on Shot Mohawk. On Shot Mohawk the fireball, which normally is unobstructed, was heavily obscured by a cloud cover so that the thermal energy at the aircraft position was reflected and diffused.

The 160-degree calorimeters mounted on the horizontal surfaces agreed well with each other. An order-of-magnitude comparison obtained by computing the vertical component of the radiant exposure recorded by the 160-degree-field-of-view calorim-

SECRET

eter mounted in the tail turret (aimed at the burst point) showed close agreement with the values recorded on the horizontal surface. In general, the vertical component of the radiant exposure determined from an integration of 90-degree-field-of-view radiometer mounted in the tail turret and aimed at ground zero also substantiated the two 160-degree-field-of-view calorimeters mounted to record the radiant exposure on the horizontal surface.

Shot Tewa showed the largest deviation between measured and predicted thermal energy. The radiant exposure measured on the 160-degree calorimeters on the underside of the fuselage was only 60 percent of the value which was predicted on the basis of the postshot yield. The pictures taken from the cameras in the tail turret indicated a clear atmosphere throughout the entire thermal phase. Good agreement was noted between the 160-degree horizontal calorimeters and the vertical components of both the 160-degree and 90-degree calorimeters mounted in the tail turret.

In reviewing the motion pictures taken from the tail-turret cameras some general observations have been made regarding the fireball. After the first minimum of the thermal pulse a dark annular ring exists on the outer edge of the fireball and obscures about 20 percent of the fireball diameter. This annular ring persists throughout the thermal phase and maintains about the same proportion in percent of fireball diameter. By the time that approximately 10 percent of the thermal pulse has elapsed, a definite boil has formed on the top of the fireball. This boil darkens to a black spot by the time that the peak intensity is reached and obscures a large portion of the fireball as viewed from the aircraft. The black spot remains fairly constant in proportion to the fireball and obscures approximately 15 percent of the total area including the dark annular ring and 25 percent of the bright area within the annular ring. No attempt is made to quantitatively evaluate the fireball area-intensity distribution, but the measured radiant exposures, which are generally below the predicted values, may be partially explained by this apparent obscurity of the fireball.

Shot Mohawk was unusual because the measured-reflected-radiant exposure from a direction directly away from the fireball, relative to that measured from the fireball direction, was believed to be higher than any previous shot in Operation Redwing or any other similar operation. The reflected-radiant exposure was measured by a 90-degree-field-of-view calorimeter mounted on the upper side of the forward fuselage. This high percentage of reflected radiation was believed to have been caused by atmospheric cloud conditions (Section 3.5). The oscillograph trace of the calorimeter measuring the reflected-radiant exposure went off the record at the time that the 160-degree calorimeter looking at the burst had received only 42 percent of the total radiant exposure. A reasonable reconstruction of the reflected-radiant exposure trace (by comparison with trace histories of other shots) indicates that the maximum reflected-radiant exposure could be approximated at 29 percent of the radiant exposure measured by the 160-degree calorimeter looking at the burst and 43 percent of the exposure measured by the 90-degree calorimeter looking at the burst.

The light-shielding capability of the crew-hood curtains was such that, for the radiation intensities experienced in Operation Redwing, protective goggles were not required by the crew. However, the light intensity inside the cockpit for Shot Mohawk approached the level of visual discomfort. The calorimeter installed inside the cockpit and directed forward toward the windshields showed no measurable quantity of radiant exposure until the end of the thermal phase for Shot Mohawk. At the end of the thermal phase, a slight increase was noted and was attributed to the crew-hood curtains being opened. It is expected that the crew-curtain installations would not be

SECRET

satisfactory for the energy levels which would be anticipated for actual-delivery missions.

4.4 THERMAL RESPONSE

In general, the measured-temperature rises on the wing, fuselage, and stabilizer thin-skin elements were lower than predicted for a given input. The preliminary correlation work done in the field was limited to a few checkpoints after Shots Cherokee and Zuni because the temperature rises for these shots were only about 60 percent of the predicted values. Therefore, it appeared that temperature would not be a limiting criterion for positioning. Consequently, the field work was concentrated on gust response. Increased temperature rises for subsequent shots were effected by increasing the absorptivity on selected thin-skin panels.

Subsequent to Operation Redwing, the thin-skin temperatures measured for all shots and at all thermocouple locations have been compared with computed values and found to be consistently below the temperatures which were predicted using the measured-thermal exposure and the temperature-calculation procedure in effect prior to Operation Redwing. The thin-skin-temperature-calculation procedure followed the method outlined in Reference 25.

A rather extensive series of laboratory tests have been conducted in an attempt to more thoroughly evaluate the temperature instrumentation so that measured and computed values of temperature may be brought into agreement. Tests were conducted on a number of thin-skin panels to define the distance at which the thermocouple should be from backup structure in order to indicate the true-panel temperature which is unaffected by the heat-sink effect of the backup structure. As a result of these tests, each thermocouple location was investigated, and, in general, all thermocouples were found to be free from any heat-sink influences. A second point of principal interest was the moisture proofing applied over the thermocouples and their adjacent leads. Tests conducted on thermocouple installations with light applications of the moisture-proofing sealant (a spot 0.75 inch in diameter and up to 0.03 inch in thickness) indicated a reduction of indicated temperature from true temperature of about 5 percent to 8 percent. A heavy application of sealant applied to the thermocouple (a spot 1.25 inches in diameter and up to 0.15 inch in thickness) resulted in a significant degrading of the indicated-panel temperature. Test-panel temperatures indicated by the thermocouples with heavy coatings of sealant were only 60 percent to 80 percent of the proper values. As indicated in Section 4.1, the actual quantity of sealant on the aircraft installations for Operation Redwing is not known.

Instrumentation was installed to evaluate convective cooling by comparing the temperature rise of a metallic slug shielded from the airstream to the temperature rise of an unshielded thin-skin panel. The effects of convective cooling were also evaluated by the examination of the temperature decay of the thin-skin panels after the thermal input was over. The results of this investigation of the temperature data, in general, indicates an apparent convective cooling which is much greater than the analytical value during the rise of the thin-skin temperatures, and an apparent convective cooling which is less than the analytical value during the cooling phase. This observation would indicate the presence of a heat sink and would substantiate the conclusion that a sufficient quantity of waterproofing sealant was applied to the thermocouple to materially affect the accuracy of the thin-skin temperature readings. With this conclusion, a rational correlation cannot be made between measured and predicted temperatures. The temperature data shown in Tables 3.6 and 3.7 indicates the comparison between the meas-

ured values a..d the temperatures predicted by the pretest methods and measured thermal inputs.

Due to the relatively low magnitude of the radiant exposures experienced in Operation Redwing, no significant temperature and thermal-strain results were obtained from the instrumented skin-stiffener wing structure.

From the overall thermal-response results obtained from Operation Redwing, and the investigations conducted thus far in an attempt to correlate measured and analytical data, a revision to the procedures used in preparing the "B-52 Special Weapons Delivery Handbook" (Reference 1) would not be warranted.

4.5 OVERPRESSURE AND MATERIAL VELOCITY

The overpressure predictions based on official preliminary yields were relatively good as seen by comparing the predicted and measured values shown in Table 3.5. After Shot Zuni, it appeared that better prediction could be made using the WADC-modified-MIT-free-air overpressure rather than the Haskell-Brubaker data. This proved to be true except for Shot Huron where the Haskell-Brubaker data gave the closer correlation. In all cases except Shots Cherokee and Navajo, the WADC-modified-MIT method gave conservative predictions by as much as 9 percent. For Shot Cherokee, the WADC-modified-MIT data gave the closer prediction, but was unconservative by 9 percent. In all cases, the Haskell-Brubaker data was unconservative. The unconservatism of the Haskell-Brubaker data was as much as 25 percent in predicting overpressures in the range of overpressures experienced by the B-52 in Operation Redwing. The measured overpressures have been scaled to a 1 kt burst for comparison with the M-Problem and Haskell-Brubaker free-air-overpressure curves in Figure 4.1.

The slight differences in overpressure from the two methods did not appreciably affect the shock-front time-of-arrival predictions for Operation Redwing. The shock-front speed was calculated by the Rankine-Hugoniot equations, and its reciprocal was integrated with respect to time to give the shock-front location at various times after detonation. Isotime plots of the shock-front position provided a means of predicting arrival time at the aircraft. The measured shock-front velocity was determined from the atmospheric data in Table C.1, measured overpressures, and the Rankine-Hugoniot expressions. Table 3.5 shows excellent agreement between measured and predicted values of shock-front velocity. Calculated time of shock-front arrival agreed with the actual time of arrival within 5 percent. The shock-impingement angle was determined from the passage of the shoꞌ front across the pressure instrumentation as outlined in Appendix D. Predicted angles were based upon the average of the angle of the radial path and the refracted-acoustic-ray angle. A comparison of the measured and analytical values of shock angle in Table 3.5 shows good agreement. Material velocity cannot be measured directly. For Operation Redwing the magnitude of the gust velocity was determined from the measured overpressure by the Rankine-Hugoniot relationship. A cross check of the magnitude was made from the measured-gust angle and the computed change in aircraft velocity based on incremental-pressure measurements, as outlined in Appendix D. Good agreement was shown between the analytical- and measured-material velocities in Table 3.5.

4.6 OVERPRESSURE RESPONSE

The only aircraft components for which measured response to overpressure was obtained were the left-hand-inboard flap as noted in paragraph 1.5.2; the ECM radome; and the bomb-bay doors. Loads on the flap were measured at a single point by replac-

ing one of the flap-support bumpers by an instrumented bumper. The load measured
on the instrumented bumper was approximately 40 percent of the value which was com-
puted analytically. The redundancy of the flap supports would tend to make the
analytical-load assumptions and analysis conservative. However, other structural
members of the flap between the support ribs were also indicated to be critical for the
loads which were expected during Operation Redwing, and no failure occurred. A
reasonable supposition, therefore, is that the load did not develop to the magnitude
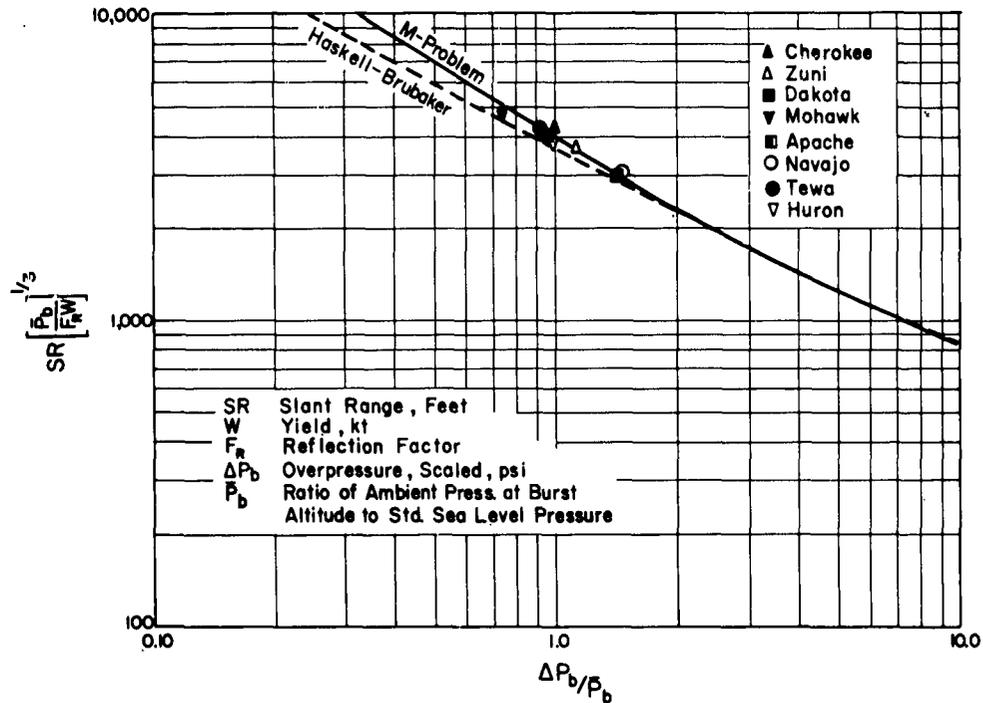
Figure 4.1 Scaled overpressure comparison.

expected. Since instrumentation to measure flap loads was added at the test site, the
system was a minimum and not elaborate enough to describe the load distribution and
time sequence.

The ECM radome was unshored during Shots Tewa and Huron in an attempt to define
the overpressure limit under dynamic conditions. The overpressure on Shot Tewa,
0.36 psi, was equal to the predicted-ultimate allowable for the radome, but no damage
was evident. However, during Shot Huron, 0.64-psi overpressure was experienced
and the radome fractured. Deflection measurements were recorded during both shots,
but the measuring system was rigged from materials available at the test site, and the
response characteristics were not satisfactory for obtaining reliable deflection data.
From the data available, the ECM-radome-ultimate overpressure is still established
at the pretest value of 0.36 psi. Figure 3.6 shows the ECM-radome damage which was
initiated by exposure to 0.64-psi overpressure.

The bomb-bay doors experienced slight buckling during Shot Huron. Considering
that the buckling was indicative of total failure, the magnification factor could be re-
duced from the pretest value of 1.67 to 1.30. The limit-allowable free-air overpressure
would then increase from 0.34 to 0.44 psi for the bomb-bay doors.

52

SECRET

4.7 WING-GUST RESPONSE

Wing Station 444 was consistently the most critical wing station. After Shots Cherokee and Zuni, the K_gD values were computed from the measured-wing loads and were found to be about 1.0 instead of the envelope value of 1.4 originally used. The value of K_gD increased with increase in altitude and the 1.4 envelope value was chosen to cover all situations up to 50,000 feet. Since test altitudes for Operation Redwing ranged from 20,000 to 41,000 feet, a K_gD value of less than 1.4 was appropriate. For the aircraft altitude in most shots, the value of 1.0 for K_gD closely approximated the analytical value. The K_gD was increased to 1.1 for Shot Tewa because of the higher aircraft altitude, 41,000 feet, where gust-alleviation effects are reduced.

The predicted-wing responses presented in Table 3.8 are computed on the basis of the K_gD values enumerated above and combined with aerodynamic characteristics observed on the airplane. The ratio of predicted to measured response on Shots Dakota and Huron indicated that a value of K_gD less than 1.0 was appropriate for these shots. Since in these two shots the aircraft altitude was lower than for the others, a reduced K_gD would be expected. Responses predicted on the basis of the methods of Reference 1, briefly described in Section 1.4.2, agree well with measured values. However, a more detailed analysis is required to properly correlate the measured response with the dynamic analysis and Reference 1 methods and is beyond the scope of this report.

4.8 STABILIZER-GUST RESPONSE

The original response predictions were based on the total stabilizer load using a combined dynamic magnification and gust-alleviation factor, K_gD, of 2.0. The magnitude of this combined value was chosen as a conservative envelope. Preliminary comparison made at the test site between measured and calculated responses indicated that the magnitude of K_gD should be approximately 1.5 and below. This decrease in K_gD from the envelope value of 2.0 did not, however, result in any increase in capability for the aircraft, because measured bending moments on the outboard portion of the Stabilizer Station 300 indicated a much more cr .cal response than the actual-total-stabilizer load.

The shift in the point of interest in stabilizer capability resulted primarily from the effect of the load impulse imposed on the stabilizer by the pressure differential resulting from the diffraction of the shock front around the stabilizer. An analysis of the time progression and duration of the overpressure impulse indicated that it is such as to excite the higher modes of the outboard-stabilizer structure, and these loads are superimposed on the gust-load increment. A detailed accounting of the various aspects of the stabilizer response requires a more elaborate presentation than is afforded by the scope of this document.

Predicted data presented in Table 3.8 for the total tail load is based on a gust increment only and a K_gD of 2.0. This is essentially the method used in the preparing of the stabilizer response data in Reference 1. It may be seen that the predicted total tail loads of Table 3.8 are quite conservative relative to the measured total tail loads.

A comparison of the left-stabilizer measured moment for Station 300 and the predicted response for total tail load shows good agreement. This is purely coincidence but indicates that the stabilizer capability presented in the weapons delivery handbook, Reference 1, will not be appreciably in error even though the stabilizer is critical for moment in the outboard region instead of total tail load.

Moment-response ratios are shown in Table 3.8 for both left and right Stabilizer

Station 300; however, moment was measured on the left side only at this station. Right-side moment ratios are considered to be realistic based on a comparison of left- and right-stabilizer-root moments. It is not known why the loads are different between the left and right sides for some shots since the gust enveloped the aircraft quite symmetrically. On Shots Mohawk, Apache, and Navajo the difference is quite apparent. The largest disagreement between left- and right-stabilizer loads occurred during Shot Mohawk when the right-stabilizer loads were approximately 35 percent higher than the left-stabilizer loads. This apparent asymmetry did not appear in calibrations either before or after Operation Redwing but such differences are observed in both the steady-state loads and dynamic loads.

4.9 OPERATIONAL CONSIDERATIONS

During Operation Redwing, the length of the single available runway at the EPG was inadequate to fulfill the requirements of the B-52. For the desired positioning accuracy, four timing runs were necessary prior to shot time. For low altitude missions, the combination of high-fuel-burn rate and low-take-off-gross weight allowed only three timing runs. Had a longer runway been available, take-off-gross weight could have been increased to allow for the desired number of timing runs.

If yields closer to that of the maximum-delivery capabilities of the participating aircraft had been detonated, several critical effects could have been measured simultaneously. During Operation Redwing, it was generally necessary, because of device yields, for the B-52 to investigate critical effects separately.

Had a shot with a more closely predictable yield been detonated during the latter part of the program, higher percentages of aircraft inputs and responses could have been attained with confidence.

Chapter 5
CONCLUSIONS and RECOMMENDATIONS

5.1 CONCLUSIONS

The objectives established for Project 5.2 in Operation Redwing were successfully accomplished. The data necessary to evaluate the existing B-52 Special Weapons Delivery Handbook were obtained, as well as other secondary information which will be useful in determining modifications pertinent to the B-52 and assisting in the design of future USAF aircraft.

It may be concluded, in general, that the vertical component of the radiant energy as measured by instruments looking at the burst and corrected by the cosine of the elevation angle is in agreement with the measurements obtained by calorimeters looking straight down.

Methods used in the B-52 Special Weapons Delivery Handbook to determine the thermal limits of the aircraft were used for predicting thermal inputs and responses of the B-52 in Operation Redwing. Based on the tentative postshot yields and actual aircraft locations, the methods of Reference 11, as employed to predict radiant exposure, were, on the average, 20 percent conservative. One shot (Zuni) was an exception, and the measured radiant exposure was 15 percent in excess of the calculated value. Based on the measured radiant exposure the thermal-response predictions were found to be conservative by approximately 30 percent, which would indicate an increase in the thermal capabilities of the B-52 to somewhat above that indicated in the delivery handbook. However, due to the method of thermocouple installation there is some question as to the accuracy of the temperature data. It is concluded that the methods used in preparing the weapons delivery handbook (Reference 1) safely predict the thermal response of the aircraft and may be quite conservative.

The analysis used in predicting the aircraft response indicated that as the structure limits are approached, the horizontal stabilizer is more critical than the wing. Tests at the EPG showed this to be true. It was found that bending at Station 300 was the most critical response on the stabilizer. Previous to Operation Redwing it was expected that total tail load was the most critical item. The capability of the stabilizer in Reference 1 was based on the total tail load but was found to be conservative and, by coincidence, sufficiently predicted the capability level of the stabilizer at Station 300.

The analytical approach to the flap-allowable overpressure was conservative. With the bumper modification which was incorporated, the flaps were capable of withstanding 100 percent of the basic aircraft-limit-allowable overpressure without damage.

Under the conditions encountered during Operation Redwing the B-52 engines operated satisfactorily and there were no indications that engine limitations were approached.

Crew-compartment thermal curtains used during the operation were found to be marginally adequate for protection from thermal radiation and flash blindness under the conditions experienced in Operation Redwing. This demonstrates a light-shielding capability which is below the energy levels anticipated for the delivery conditions established in Reference 1.

Minor thermal damage was obtained on almost every shot on such items as seals on

SECRET

the bomb-bay doors, wheel-well doors, flaps, and aileron and elevator-control tabs. The damage did not affect the flight safety of the aircraft and is not considered as a weapons-delivery limitation but may require additional maintenance.

Shot Huron demonstrated that the bomb-bay doors could withstand a free-air overpressure of approximately 0.65 psi with only slight local buckling. This is above the overpressure level to which the aircraft would be subjected under the delivery conditions of Reference 1, and it is concluded that the bomb-bay doors are satisfactory for the delivery conditions of Reference 1.

The ECM radome is the weakest component with respect to overpressure but will withstand at least 0.36 psi. The ECM-radome capability is below the overpressure-capability level to which the aircraft would be subjected under the delivery conditions of Reference 1.

Nuclear radiation was insignificant for the B-52 locations relative to the detonation points.

5.2 RECOMMENDATIONS

The following recommendations are a result of the experience gained by Project 5.2 in Operation Redwing:

1. The B-52 need not participate in future nuclear tests as weapon-capability aircraft under the delivery conditions stated in the present B-52 Special Weapons Delivery Handbook.

2. It is recommended that the data obtained during Operation Redwing, as well as from previous operations, be used to develop or modify existing theories into more expeditious and less complex methods of predicting blast- and thermal-energy levels in space. These new or modified methods should not, however, sacrifice accuracy for simplicity.

3. It is recommended that the thermal crew curtains and curtain installations be evaluated to develop a curtain and installation which will provide a satisfactory light-shielding capability for anticipated energy levels as determined for the Reference 1 delivery conditions.

4. It is recommended that revisions be made to the ECM radome to increase its overpressure capability to be consistent with the basic overpressure capability of the B-52.

SECRET

Appendix A

PROJECT 5.2 ORGANIZATION

SECRET
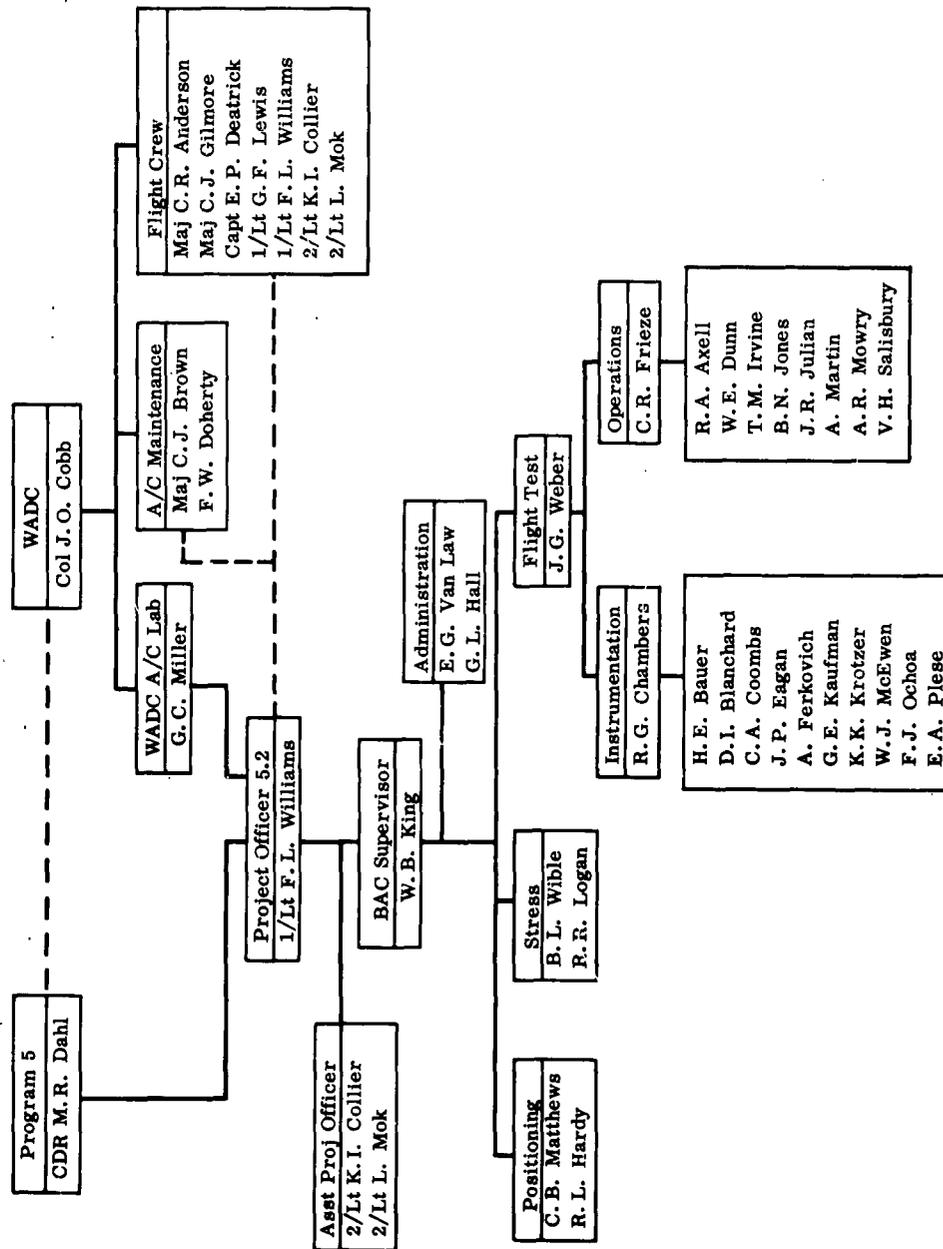
Figure A.1 Project 5.2 organization and relationship with Program 5 and the WADC Effects Element.

58

Appendix B

INSTRUMENTATION LOCATIONS

Figures B.1 through B.9 show the locations of instrumentation in the various components
of B-52 Serial No. 52-004.

SECRET
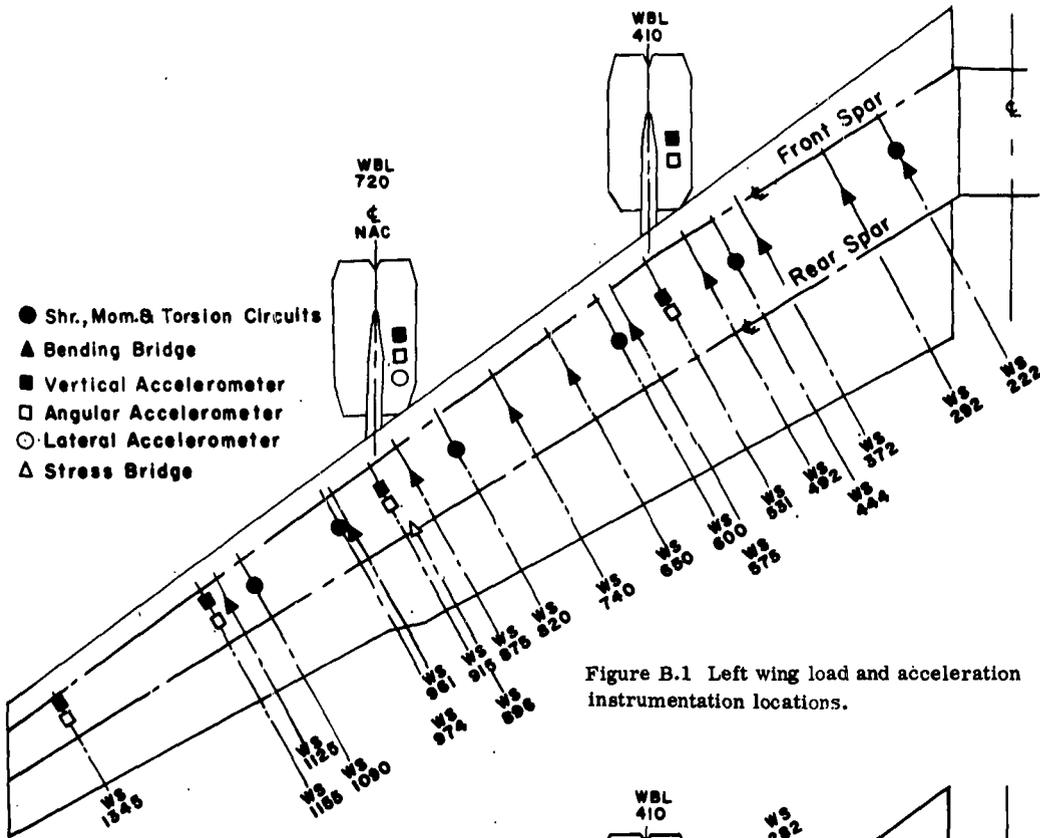
Figure B.1 Left wing load and acceleration instrumentation locations.

Legend:
- ● Shr., Mom.& Torsion Circuits
- ▲ Bending Bridge
- ■ Vertical Accelerometer
- □ Angular Accelerometer
- ○ Lateral Accelerometer
- △ Stress Bridge

Legend:
- ○ Thermocouple—Upr Surface
- ● Thermocouple—Lwr Surface
- □ Covered Thermocouple
- △ Stress Bridge—Upr Surface
- ▲ Stress Bridge—Lwr Surface
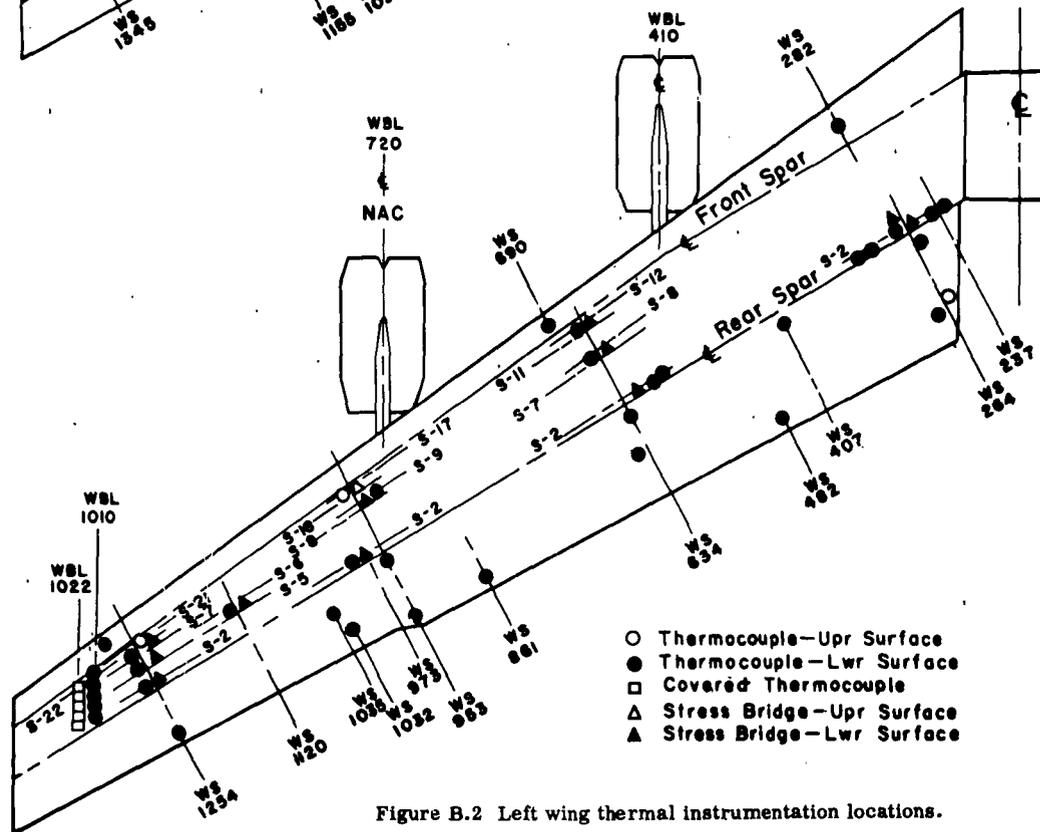
Figure B.2 Left wing thermal instrumentation locations.

60

SECRET
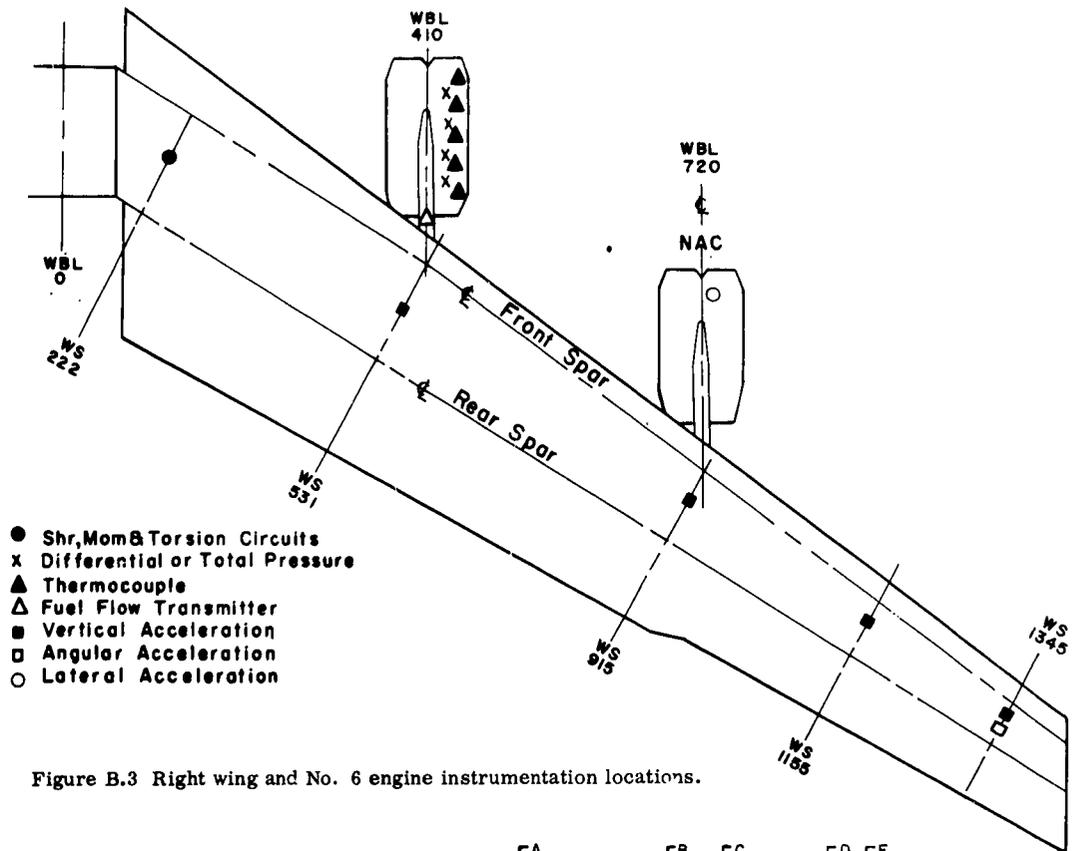
Figure B.3 Right wing and No. 6 engine instrumentation locations.

- ● Shr,Mom&Torsion Circuits
- x Differential or Total Pressure
- ▲ Thermocouple
- △ Fuel Flow Transmitter
- ■ Vertical Acceleration
- □ Angular Acceleration
- ○ Lateral Acceleration

P_{T2} Inlet Total Pressure

P_{T3} Intercompressor Total Pressure

P_{T4} Compressor Discharge Total Pressure

P_{T7} Turbine Discharge Total Pressure

T_{T2} Inlet Total Temperature

T_{T3} Intercompressor Total Temperature

T_{T4} Compressor Discharge Total Temperature

T_{T5} Turbine Inlet Total Temperature

T_{T7} Turbine Discharge Total Temperature (4 Thermocouples Parallel)

Figure B.4 No. 6 engine instrumentation locations.

61

Legend:

○ Vertical Acceleration   v Shear
◐ Angular Acceleration   M Moment
● Lateral Acceleration   T Torsion
▲ Stress Bridge
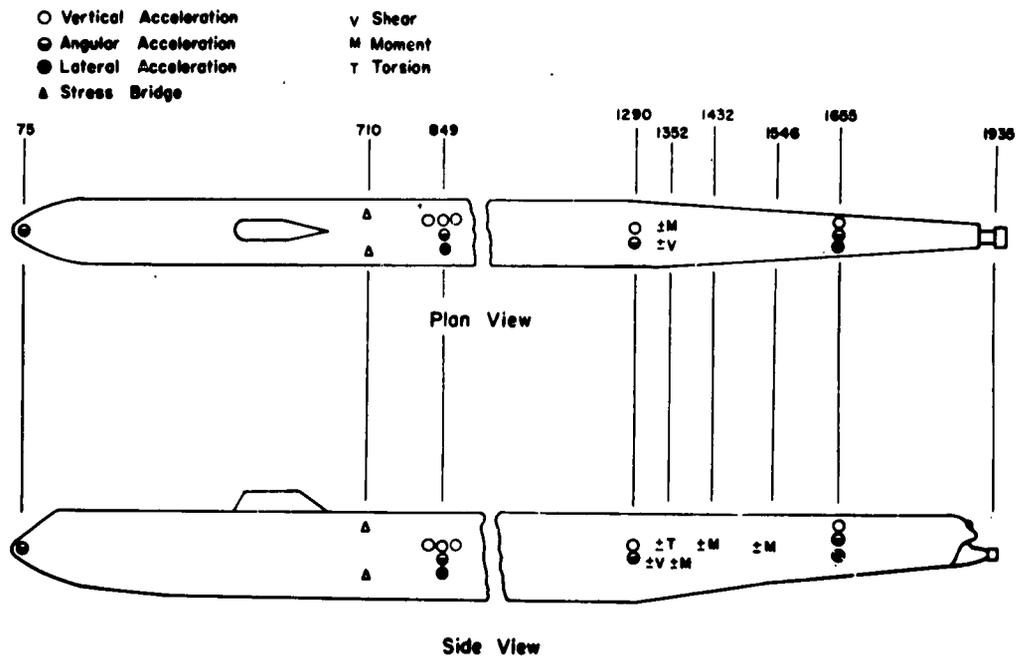
Figure B.5 Fuselage load and acceleration instrumentation locations.

Legend:

● Thermocouple   ○ Calorimeter
□ Pressure Pickup   △ Radiometer
■ Camera   Symbol Script Indicates Quantity
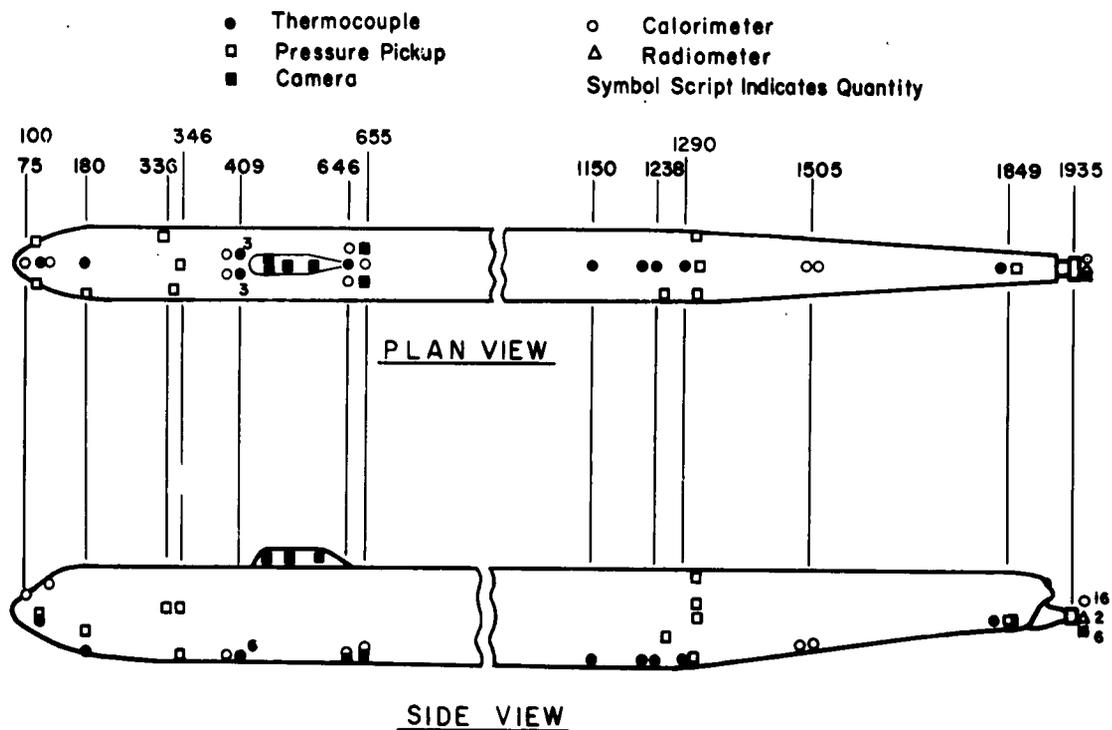
Figure B.6 Fuselage thermal and pressure instrumentation and camera locations.

62

SECRET
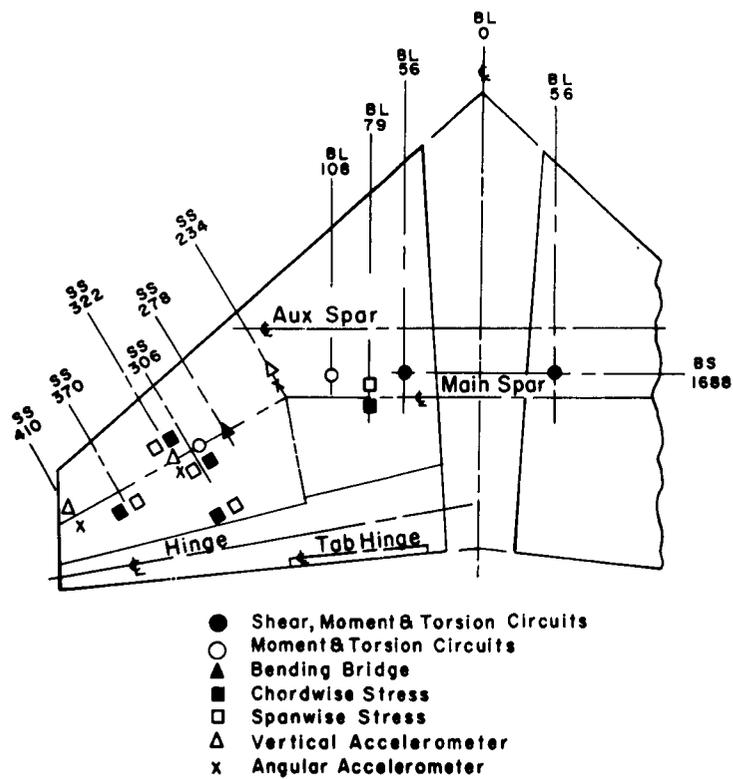
Figure B.7 Horizontal stabilizer load and acceleration instrumentation locations.
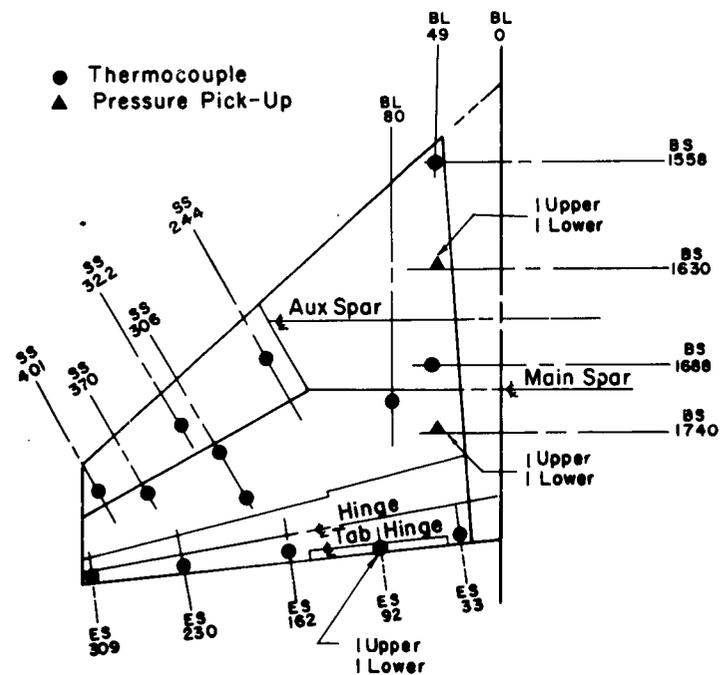
Figure B.8 Horizontal stabilizer thermal and pressure instrumentation locations.

63

SECRET
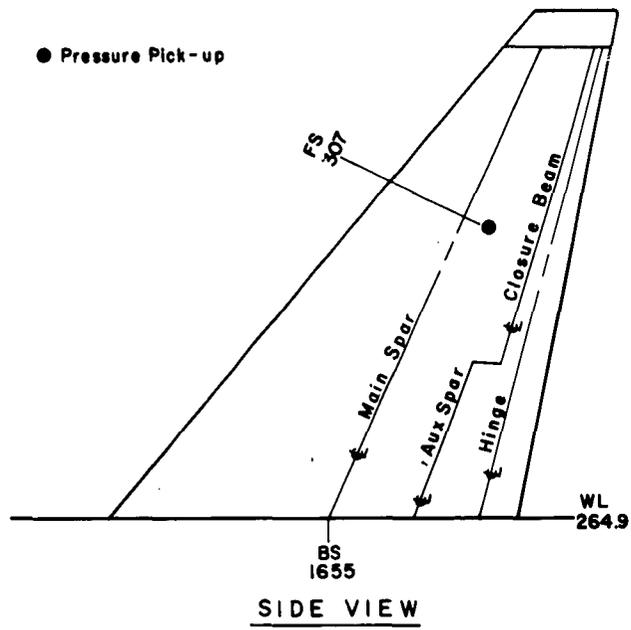
Figure B.9 Vertical fin pressure instrumentation location.

Appendix C
METEOROLOGICAL DATA

Table C.1 shows meteorological data relative to the test shots in which B-52 Serial No. 52-004 participated.

TABLE C.1 METEOROLOGICAL DATA

Observed weather furnished by Joint Task Force Seven.

Shot	Conditions at Sea Level			Aircraft Absolute Altitude	Conditions at Aircraft Absolute Altitude			
	Pressure	Temperature	Humidity		Pressure	Temperature	Wind Velocity	Wind Direction
	mb	F	pct	kilofeet	mb	F	knots	deg
Cherokee	1,009.0	81.0	76	31	307	−26.0	06	235
Zuni	1,010.5	81.0	80	32	295	−28.8	27	210
Dakota	1,009.1	82.0	80	22	441	6.0	10	220
Mohawk	1,010.2	79.6	81	25	396	1.6	05	160
Apache	1,010.5	80.3	84	34	270	−38.8	15	200
Navajo	1,010.2	81.2	80	38	225	−58.5	15	260
Tewa	1,009.3	82.0	85	41	194	−74.0	20	260
Huron	1,007.8	81.4	84	20	483	−18.5	06	020

65

Appendix D
MISCELLANEOUS DERIVATIONS

D.1 SHOCK-FRONT VELOCITY AND ANGLE

Three pressure transducers, at widely spaced locations on the aircraft, were used to determine the shock-front velocity and angle. The equations for calculating these quantities, using the measured times required for the shock to traverse the instruments, are developed below. It is assumed that there is no yaw angle between the aircraft and shock-velocity vectors, so a two-dimensional analysis is used.

The geometry of the instrument locations and the shock front at the time when the first instrument is affected is shown in Figure D.1.

Where: V_a = velocity of airplane (true), ft/sec

V_s = velocity of shock front, ft/sec

V_{sa} = relative velocity of shock front with respect to the airplane, ft/sec

Δt_1 = time required for shock to travel from Gage 1 to Gage 2, sec

Δt_2 = time required for shock to travel from Gage 1 to Gage 3, sec

η = angle between the shock-front-velocity vector and the horizontal, deg

γ = pitch angle of the aircraft, deg

ϕ = angle between a water line and the reference line connecting pressure ports P_1 and P_3, deg

From Figure D.1:

$$V_s = V_{sa} \sin \tau + V_a \cos \eta$$

$$a \sin \theta = d_2 \sin \tau$$

$$d_2 = V_{sa} \Delta t_2$$

Therefore, by substitution the equation for the shock-front velocity is:

$$V_s = \frac{a \sin \theta}{\Delta t_2} + V_a \cos \eta$$

The angle of the shock-front velocity is calculated from

$$\eta = 90 - \theta - \delta$$

Where, from Figure D.1,

$$\delta = \phi + \gamma$$

The remaining unknown in the equations of shock-front velocity and angle is the angle θ which is defined from Figure D.1 as:

$$\theta = \operatorname{ctn}^{-1}\left[\frac{\dfrac{a}{b} \times \dfrac{\Delta t_1}{\Delta t_2} - \cos\sigma}{\sin\sigma}\right]$$
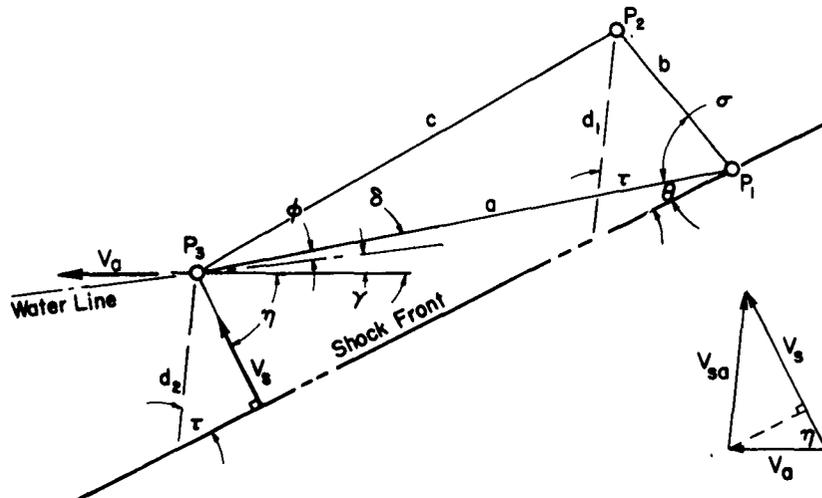
Figure D.1 Pressure instrument and shock front geometry.

D.2 POSTSHOCK AIRCRAFT TRUE AIRSPEED

The postshock true airspeed may be computed in terms of the properties of the atmosphere and the preshock airspeed as derived below.

Let P_T = total pressure, psi

P = ambient pressure, psi

γ = ratio of specific heats for air, 1.4

V = aircraft true airspeed, ft/sec

a = speed of sound, ft/sec

ξ = pressure ratio P_2/P_1

and subscripts 1 and 2 refer to preshock and postshock conditions, respectively.

From Bernoulli's equation of isentropic flow in a compressible fluid:

$$V = \left\{\left[\left(\frac{P_T}{P}\right)^{\frac{\gamma-1}{\gamma}} - 1\right]\frac{2a^2}{\gamma-1}\right\}^{1/2}$$

Then by ratio of the preshock and postshock conditions, the postshock aircraft velocity may be determined from,

67

SECRET

$$\frac{V_2}{V_1} = \frac{a_2}{a_1} \left[\frac{\left(\frac{P_{T_2}}{P_2}\right)^{\frac{\gamma-1}{\gamma}} - 1}{\left(\frac{P_{T_1}}{P_1}\right)^{\frac{\gamma-1}{\gamma}} - 1} \right]^{1/2}$$

Where the postshock parameters necessary to perform the calculation may be determined from preshock quantities as:

$$P_2' = P_1 + \Delta P$$

$$P_{T_2} = P_{T_1} + \Delta P_T$$

$$\frac{a_2}{a_1} = \left\{ \xi \left[\frac{\xi + \left(\frac{\gamma+1}{\gamma-1}\right)}{\xi \left(\frac{\gamma+1}{\gamma-1}\right) + 1} \right] \right\}^{1/2} \qquad \text{(Rankine-Hugoniot relationship)}$$

The incremental pressures ΔP and ΔP_T were measured from a high-response-rate pressure system.

The preshock value of the total pressure, P_{T_1}, may be calculated from the Bernoulli equation rearranged as

$$P_{T_1} = P_1 \left[1 + \frac{\gamma-1}{2} \left(\frac{V}{a}\right)^2 \right]^{\frac{\gamma}{\gamma-1}}$$

but, $\qquad a = 49.01 \sqrt{T} \qquad$ and, $\quad \gamma = 1.4$

so, $\qquad P_{T_1} = P_1 \left[1 + \frac{0.83275 \times 10^{-4}}{T} V^2 \right]^{3.5}$

D.3 MATERIAL VELOCITY DETERMINED FROM AIRCRAFT VELOCITIES AND SHOCK ANGLE

The material velocity may be calculated using the preshock aircraft velocity, the postshock aircraft velocity as calculated in Appendix D.2, and the shock-front angle as calculated in Appendix D.1.
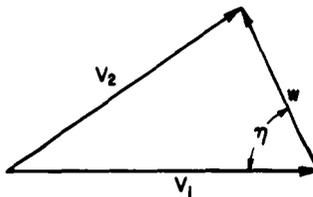
By geometry from the above diagram,

SECRET

$$w = \sqrt{V_2{}^2 - V_1{}^2 \sin^2 \eta} + V_1 \cos \eta$$

Where: w = material velocity, ft/sec

V = aircraft velocity, ft/sec

η = angle of shock front, deg

and subscripts 1 and 2 refer to preshock and postshock, respectively.

SECRET

REFERENCES

1. "B-52 Special Weapons Delivery Handbook"; April 1956; WADC Technical Report 56-81; Secret Restricted Data.

2. "The Effects of Atomic Explosions on Aircraft"; January 1953; WADC Technical Report 52-244; Secret Restricted Data.

3. J. C. Wayne and J. C. Lehmkuhl; "Blast Effects on Aircraft in Flight"; Operation Greenhouse Report No. 99, Annex 8.1 to the Scientific Director's Report; October 1951; Aircraft Laboratory of the Aeronautical Division, WADC; Secret Restricted Data.

4. "Preliminary Results of Nuclear Weapons Effects on Aircraft"; Operation Ivy; January 1953; Allied Research Associates Document No. 125; Secret Restricted Data.

5. G. F. Purkey; "Blast Effects on B-36 Type Aircraft in Flight"; Project 5.3, Operation Upshot-Knothole, WT-750, March 1955; Aircraft Laboratory, Wright Air Development Center, Dayton, Ohio; Secret Restricted Data.

6. G. C. Miller, E. J. Schlei and C. R. Andrews; "Blast and Thermal Effects on B-36 Aircraft in Flight"; Project 6.2a, Operation Castle, WT-925, June 1956; Aircraft Laboratory, Wright Development Center, Dayton, Ohio; Confidential Formerly Restricted Data.

7. C. W. Brenner and others; "Handbook for the Computation of Danger Regions for B-36J Airplane Subjected to the Thermal and Blast Effects of a Nuclear Detonation"; September 1955; WADC Technical Note 55-173; Secret Restricted Data.

8. D. J. Fink and J. M. Kane; "Handbook for the Computation of Dynamic Gust Loads Received by a B-50D Airplane Subjected to the Shock Wave of a Nuclear Explosion"; July 1953; WADC Technical Report 53-176; Secret Restricted Data.

9. C. W. Luchsinger; "Thermal Effects on B-47B Aircraft in Flight"; Project 6.2b, Operation Castle, WT-926, April 1957; Wright Air Development Center, Dayton, Ohio; Secret Formerly Restricted Data.

10. C. W. Brenner, M. R. Rubin and E. I. Gray; "Handbook for the Computation of Danger Regions for a B-47E Airplane Subjected to the Thermal and Blast Effects of a Nuclear Detonation"; September 1955; WADC Technical Note 55-175; Secret Restricted Data.

11. R. M. Chapman and M. H. Seavey; "Preliminary Report on the Attenuation of Thermal Radiation from Atomic or Thermonuclear Weapons"; November 1954; Air Force Cambridge Research Center Technical Note 54-25; Secret Restricted Data.

12. "Special Weapons Delivery Capabilities, B-52"; May 1954; Boeing Airplane Company Document D-15113; Secret Restricted Data.

13. N. A. Haskell and R. M. Brubaker; "Free Air Atomic Blast Pressure Measurements"; Project 1.3, Operation Upshot-Knothole, November 1953; Air Force Cambridge Research Center Technical Report 54-20; Secret Restricted Data.

SECRET

14. J. C. Ledsham and H. H. M. Pike; "The Effects of Atmospheric Variations on the Propagation of Blast Waves to High Altitudes"; January 1951; Armament Research Establishment, Ministry of Supply, ARE Report No. 31/50; Secret Restricted Data.

15. "Project 004 Thermal Tests"; February 1956; Boeing Airplane Company Test Report T-29654; Unclassified.

16. "Thermal Capabilities of Materials, B-52 Special Delivery Capability, Phase II"; April 1956; Boeing Airplane Company Test Report T-29599; Unclassified.

17. "Section Q, Fuselage Negative Pressure Tests"; February 1955; Boeing Airplane Company Test Report T-25523; Unclassified.

18. "Flaps, Aileron, and Airbrake Stress Analysis, XB-52 and B-52"; 30 April 1951; Boeing Airplane Company Document D-11377; Unclassified.

19. "Ground Calibration for Flight Load Survey, AF 52-004 "; May 1955; Boeing Airplane Company Document D-16828; Unclassified.

20. "Flight Load Survey and Structural Integrity Flight Demonstration, Airplane AF 52-004"; May 1956; Boeing Airplane Company Document D-17315; Confidential.

21. "Fuselage Stress Analysis, XB-52 and B-52"; 1954; Boeing Airplane Company Document D-11373; Unclassified.

22. J. R. Alexander; "A Modified Method for Computation of Overpressure and Overpressure Envelopes"; May 1955; WADC Technical Note WCLS 55-13; Secret Restricted Data.

23. "B-52B, Operation Redwing Data"; WADC TN 56-446.

24. "Portable Reflectometer Instruction Manual"; January 1956; Boeing Airplane Company Document D-17790; Unclassified.

25. "Temperature Distributions in a Typical Aircraft Structure Due to Transient External Heating"; April 1953; WADC Technical Report 52-216; Confidential.

26. Richard R. Henldenfels; "The Effect of Non-Uniform Temperature Distribution on the Stresses and Distortions of Stiffened-Shell Structures"; November 1950; NACA TN 2240; Unclassified.

SECRET

DISTRIBUTION

Military Distribution Category 52

ARMY ACTIVITIES

1   Deputy Chief of Staff for Military Operations, D/A, Washington 25, D.C. ATTN: Dir. of SW&R
2   Chief of Research and Development, D/A, Washington 25, D.C. ATTN: Atomic Div.
3   Assistant Chief of Staff, Intelligence, D/A, Washington 25, D.C.
4   Chief of Engineers, D/A, Washington 25, D.C. ATTN: ENGTB
5- 6   Office, Chief of Ordnance, D/A, Washington 25, D.C. ATTN: ORDTN
7   Chief of Transportation, D/A, Office of Planning and Int., Washington 25, D.C.
8- 10   Commanding General, U.S. Continental Army Command, Ft. Monroe, Va.
11   Director of Special Weapons Development Office, Head-quarters CONARC, Ft. Bliss, Tex. ATTN: Capt. Chester I. Peterson
12   President, U.S. Army Artillery Board, Ft. Sill, Okla.
13   President, U.S. Army Air Defense Board, Ft. Bliss, Tex.
14   President, U.S. Army Aviation Board, Ft. Rucker, Ala. ATTN: ATBG-DG
15   Commandant, U.S. Army Command & General Staff College, Ft. Leavenworth, Kansas. ATTN: ARCHIVES
16   Commandant, U.S. Army Air Defense School, Ft. Bliss, Tex. ATTN: Dept. of Tactics and Combined Arms
17   Commandant, U.S. Army Artillery and Missile School, Ft. Sill, Okla. ATTN: Combat Development Department
18   Commandant, U.S. Army Aviation School, Ft. Rucker, Ala.
19   Commandant, U.S. Army Ordnance School, Aberdeen Proving Ground, Md.
20   Commandant, U.S. Army Ordnance and Guided Missile School, Redstone Arsenal, Ala.
21   Commanding General, U.S. Army Chemical Corps, Research and Development Comd., Washington 25, D.C.
22- 23   Commanding Officer, Chemical Warfare Lab., Army Chemical Center, Md. ATTN: Tech. Library
24   Commanding Officer, Diamond Ord. Fuze Labs., Washington 25, D.C. ATTN: Chief, Nuclear Vulnerability Br. (230)
25- 26   Commanding General, Aberdeen Proving Grounds, Md. ATTN: Director, Ballistics Research Laboratory
27- 28   Commanding General, U.S. Army Ord. Missile Command, Redstone Arsenal, Ala.
29   Commander, Army Rocket and Guided Missile Agency, Red-stone Arsenal, Ala. ATTN: Tech Library
30   Commanding General, White Sands Proving Ground, Las Cruces, N. Mex. ATTN: ORDBS-OM
31   Commander, Army Ballistic Missile Agency, Redstone Arsenal, Ala. ATTN: ORDAB-HT
32   Commanding General, Ordnance Ammunition Command, Joliet, Ill.
33   Commanding Officer, USA Transportation R&E Comd., Ft. Eustis, Va. ATTN: Chief, Tech. Svcs. Div.
34   Commanding Officer, USA Transportation Combat Development Group, Ft. Eustis, Va.
35   Director, Operations Research Office, Johns Hopkins University, 6935 Arlington Rd., Bethesda 14, Md.
36   Commander-in-Chief, U.S. Army Europe, APO 403, New York, N.Y. ATTN: Opot. Div., Weapons Br.

NAVY ACTIVITIES

37   Chief of Naval Operations, D/N, Washington 25, D.C. ATTN: OP-03EG
38   Chief of Naval Operations, D/N, Washington 25, D.C. ATTN: OP-75
39   Chief of Naval Operations, D/N, Washington 25, D.C. ATTN: OP-92201
40- 41   Chief of Naval Research, D/N, Washington 25, D.C. ATTN: Code 811

42- 43   Chief, Bureau of Aeronautics, D/N, Washington 25, D.C.
44- 48   Chief, Bureau of Aeronautics, D/N, Washington 25, D.C. ATTN: AER-AD-41/20
49   Chief, Bureau of Ordnance, D/N, Washington 25, D.C.
50   Chief, Bureau of Ordnance, D/N, Washington 25, D.C. ATTN: S.P.
51   Director, U.S. Naval Research Laboratory, Washington 25, D.C. ATTN: Mrs. Katherine H. Cass
52- 53   Commander, U.S. Naval Ordnance Laboratory, White Oak, Silver Spring 19, Md.
54   Director, Material Lab. (Code 900), New York Naval Shipyard, Brooklyn 1, N.Y.
55   Commanding Officer, U.S. Naval Mine Defense Lab., Panama City, Fla.
56- 57   Commanding Officer, U.S. Naval Radiological Defense Laboratory, San Francisco, Calif. ATTN: Tech. Info. Div.
58   Commanding Officer, U.S. Naval Schools Command, U.S. Naval Station, Treasure Island, San Francisco, Calif.
59   Superintendent, U.S. Naval Postgraduate School, Monterey, Calif.
60   Commanding Officer, Nuclear Weapons Training Center, Atlantic, U.S. Naval Base, Norfolk 11, Va. ATTN: Nuclear Warfare Dept.
61   Commanding Officer, Nuclear Weapons Training Center, Pacific, Naval Station, San Diego, Calif.
62   Commanding Officer, U.S. Naval Damage Control Tng. Center, Naval Base, Philadelphia 12, Pa. ATTN: ABC Defense Course
63   Commanding Officer, Air Development Squadron 5, VX-5, China Lake, Calif.
64   Director, Naval Air Experiment Station, Air Material Center, U.S. Naval Base, Philadelphia, Pa.
65   Commander, Officer U.S. Naval Air Development Center, Johnsville, Pa. ATTN: NAS, Librarian
66   Commanding Officer, Naval Air Sp. Wpns. Facility, Kirtland AFB, Albuquerque, N. Mex.
67   Commander, U.S. Naval Ordnance Test Station, China Lake, Calif.
68- 71   Commandant, U.S. Marine Corps, Washington 25, D.C. ATTN: Code A03H
72   Commanding Officer, U.S. Naval CIC School, U.S. Naval Air Station, Glynco, Brunswick, Ga.

AIR FORCE ACTIVITIES

73   Assistant for Atomic Energy, HQ, USAF, Washington 25, D.C. ATTN: DCS/O
74   Deputy Chief of Staff, Operations HQ. USAF, Washington 25, D.C. ATTN: Operations Analysis
75- 76   Assistant Chief of Staff, Intelligence, HQ. USAF, Washington 25, D.C. ATTN: AFCIN-3B
77   Director of Research and Development, DCS/D, HQ. USAF, Washington 25, D.C. ATTN: Guidance and Weapons Div.
78   The Surgeon General, HQ. USAF, Washington 25, D.C. ATTN: Bio.-Def. Pre. Med. Division
79   Commander, Tactical Air Command, Langley AFB, Va. ATTN: Doc. Security Branch
80   Commander, Air Defense Command, Ent AFB, Colorado. ATTN: Atomic Energy Div., ADLAN-A
81   Commander, Hq. Air Research and Development Command, Andrews AFB, Washington 25, D.C. ATTN: RDRWA
82   Commander, Air Force Ballistic Missile Div. HQ. ARDC, Air Force Unit Post Office, Los Angeles 45, Calif. ATTN: WDSOT
83- 84   Commander, AF Cambridge Research Center, L. G. Hanscom Field, Bedford, Mass. ATTN: CRQST-2
85- 89   Commander, Air Force Special Weapons Center, Kirtland AFB, Albuquerque, N. Mex. ATTN: Tech. Info. & Intel. Div.
90- 91   Director, Air University Library, Maxwell AFB, Ala.

73

92	Commander, Lowry AFB, Denver, Colorado. ATTN: Dept. of Sp. Wpns. Tng.
93	Commandant, School of Aviation Medicine, USAF, Randolph AFB, Tex. ATTN: Research Secretariat
94	Commander, 1009th Sp. Wpns. Squadron, HQ. USAF, Washington 25, D.C.
95- 97	Commander, Wright Air Development Center, Wright-Patterson AFB, Dayton, Ohio. ATTN: WCOSI
98- 99	Director, USAF Project RAND, VIA: USAF Liaison Office, The RAND Corp., 1700 Main St., Santa Monica, Calif.
100	Commander, Air Defense Systems Integration Div., L. G. Hanscom Field, Bedford, Mass. ATTN: SIDE-S
101	Chief, Ballistic Missile Early Warning Project Office, 220 Church St., New York 13, N.Y. ATTN: Col. Leo V. Skinner, USAF
102	Commander, Air Technical Intelligence Center, USAF, Wright-Patterson AFB, Ohio. ATTN: AFCIN-4B1a, Library
103	Assistant Chief of Staff, Intelligence, HQ. USAFE, APO 633, New York, N.Y. ATTN: Directorate of Air Targets
104	Commander-in-Chief, Pacific Air Forces, APO 953, San Francisco, Calif. ATTN: PFCIE-MB, Base Recovery

OTHER DEPARTMENT OF DEFENSE ACTIVITIES

105	Director of Defense Research and Engineering, Washington 25, D.C. ATTN: Tech. Library
106	Director, Weapons Systems Evaluation Group, Room 1E880, The Pentagon, Washington 25, D.C.
107-114	Chief, Defense Atomic Support Agency, Washington 25, D.C. ATTN: Document Library

115	Commander, Field Command, DASA, Sandia Base, Albuquerque, N. Mex.
116	Commander, Field Command, DASA, Sandia Base, Albuquerque, N. Mex. ATTN: FCTG
117-121	Commander, Field Command, DASA, Sandia Base, Albuquerque, N. Mex. ATTN: FCWT
122	Administrator, National Aeronautics and Space Administration, 1520 "H" St., N.W., Washington 25, D.C. ATTN: Mr. R. V. Rhode
123	Commander-in-Chief, Strategic Air Command, Offutt AFB, Neb. ATTN: OAWS
124	Commander-in-Chief, APO 128, New York, N.Y.

ATOMIC ENERGY COMMISSION ACTIVITIES

125-127	U.S. Atomic Energy Commission, Technical Library, Washington 25, D.C. ATTN: For DMA
128-129	Los Alamos Scientific Laboratory, Report Library, P.O. Box 1663, Los Alamos, N. Mex. ATTN: Helen Redman
130-134	Sandia Corporation, Classified Document Division, Sandia Base, Albuquerque, N. Mex. ATTN: H. J. Smyth, Jr.
135-137	University of California Lawrence Radiation Laboratory, P.O. Box 808, Livermore, Calif. ATTN: Clovis G. Craig
138	Essential Operating Records, Division of Information Services for Storage at ERC-H. ATTN: John R. Hans, Chief, Headquarters Records and Mail Service Branch, U.S. AEC, Washington 25, D.C.
139	Weapon Data Section, Technical Information Service Extension, Oak Ridge, Tenn.
140-170	Technical Information Service Extension, Oak Ridge, Tenn. (Surplus)